# Clinical Outcomes of Phototherapeutic Keratectomy in Eyes With Thiel-Behnke Corneal Dystrophy

OSAMU HIEDA, SATOSHI KAWASAKI, KOUICHI WAKIMASU, KENTA YAMASAKI, TSUTOMU INATOMI, AND SHIGERU KINOSHITA

• PURPOSE: To investigate the functional and morphologic midterm outcome of phototherapeutic keratectomy (PTK) for Thiel-Behnke corneal dystrophy diagnosed by gene-mutation analysis.

• DESIGN: Retrospective, single-center clinical study.

• METHODS: Between July 2001 and May 2010, 10 consecutive PTKs were performed in 10 eyes of 5 patients (2 male, 3 female; mean age: 55 ± 13 years) with superficially accentuated opacities caused by Thiel-Behnke corneal dystrophy and were followed up for at least 12 months (range: 12–108 months). Main outcome measures included (1) best-corrected visual acuity (BCVA), (2) uncorrected visual acuity (UCVA), (3) spherical equivalent, and (4) recurrence rate. The probability of recurrence of Thiel-Behnke corneal dystrophy after PTK was calculated using the Kaplan-Meier method for survival analysis.

• RESULTS: The p.Arg555Gln mutation was found within the *TGFBI* gene in all 5 patients. Average logarithm of minimal angle of resolution (logMAR) BCVA change was −0.55 ± 0.26. Average logarithm UCVA change was −0.54 ± 0.31. In 5 of the 10 eyes, recurrence of central superficial opacification was clinically identified during the follow-up periods, and in 4 of those 5 eyes, the level of the recurrence was so significant that the visual acuity was reduced more than 2 lines. The maximum follow-up period of the 1 eye without significant post-PTK recurrence was 108 months.

• CONCLUSIONS: PTK is a successful therapy for Thiel-Behnke corneal dystrophy, and results in midterm stable visual acuity and corneal transparency. Unlike in Reis-Bücklers corneal dystrophy cases, PTK delays the need for more invasive surgical intervention in Thiel-Behnke corneal dystrophy. (Am J Ophthalmol 2013;155: 66–72. © 2013 by Elsevier Inc. All rights reserved.)

Accepted for publication Jun 25, 2012.

From the Department of Ophthalmology, Kyoto Prefectural University of Medicine, Kyoto, Japan (O.H., Sa.K., T.I., Sh.K.); Baptist Eye Clinic, Kyoto, Japan (K.W.); and Department of Biomedical Engineering, Faculty of Life and Medical Sciences, Doshisha University, Kyotanabe, Japan (K.Y.).

Inquiries to Osamu Hieda, Department of Ophthalmology, Kyoto Prefectural University of Medicine, 465 Kajii-cho, Hirokoji-agaru, Kawaramachi-dori, Kamigyo-ku, Kyoto 602-0841, Japan; e-mail: ohieda@koto.kpu-m.ac.jp

THIEL-BEHNKE CORNEAL DYSTROPHY,[1] ALSO KNOWN as "honeycomb" corneal dystrophy,[2] is an autosomal dominant inheritable disease and was described as corneal dystrophy of the Bowman layer and superficial stroma type II (CDB II, OMIM#602082) in a report by Küchle and associates.[3] Recent molecular biological analysis has revealed that this dystrophy is caused by the missense mutation (p.Arg555Gln) of the human transforming growth factor beta–induced (*TGFBI*) gene.[2,4–7]

Characteristic bilateral, subepithelial corneal opacities, frequently accompanied by recurrent corneal erosions, normally appear in Thiel-Behnke corneal dystrophy patients between the ages of 10 and 20 years. This disease runs a slow progressive course, with painful erosive episodes and gradual deterioration of vision.[2–4] The treatment modalities for this disease include superficial keratectomy, lamellar keratoplasty,[3] penetrating keratoplasty (PKP),[8] and phototherapeutic keratectomy (PTK).[9–12]

In Japan, the Ministry of Health, Labour and Welfare approved the medical use of 193-nm argon-fluoride excimer laser devices for PTK procedures in 2000. Since then, PTK has been applied for the treatment of various types of corneal diseases, including inheritable corneal dystrophies,[2,12–17] band keratopathy,[10,18–20] recurrent corneal erosion,[15,21,22] certain types of degenerative corneal diseases (eg, Salzmann's degeneration),[10,20,23] and bullous keratopathy.[24,25] The PTK procedure is generally thought to produce the best results when it is used for the ablation of corneal opacity restricted to the anterior stroma of the cornea. When PTK is performed on patients who have passed strict diagnostic criteria, the satisfaction level in relation to the results of this procedure is reportedly very high.[26]

The purpose of this retrospective, single-center clinical study was to investigate the functional and morphologic midterm outcome of PTK performed in multiple Thiel-Behnke corneal dystrophy patients who were strictly diagnosed through the use of gene mutation analysis.

## METHODS

• STUDY POPULATION: This study involved 10 consecutive PTKs performed in 10 eyes (5 right eyes and 5 left eyes) of 5 patients (2 male and 3 female) to treat superficially accentuated opacities that were clinically and





0002-9394/$36.00
http://dx.doi.org/10.1016/j.ajo.2012.06.022

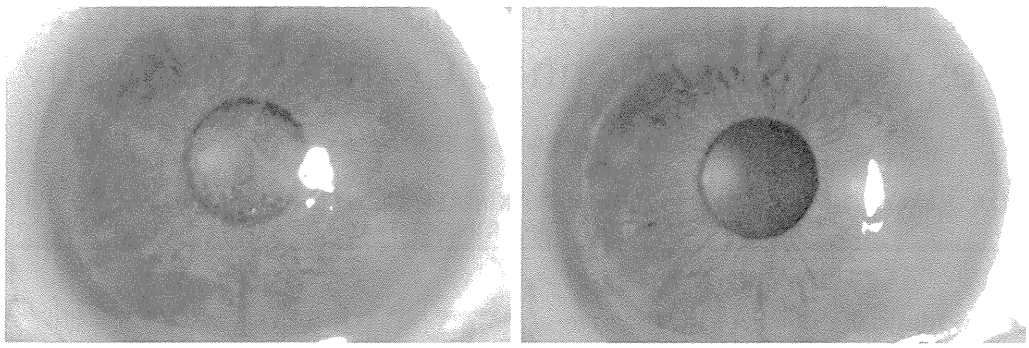

FIGURE 1. Slit-lamp microscopy images of the left eye of a 57-year-old woman with Thiel-Behnke corneal dystrophy (Patient 1) (Left) before and (Right) 1 month after undergoing phototherapeutic keratectomy surgery. Note that the superficial corneal opacities visible around the axial area of the cornea in the left-hand image (presurgery) are no longer visible in the right-hand image (postsurgery).

**TABLE.** Summarized Clinical Information of Eyes With Thiel-Behnke Corneal Dystrophy Before and After Phototherapeutic Keratectomy

| | | | | BCVA (logMAR) | | | (Month) | |
|---|---|---|---|---|---|---|---|---|
| Patient[a] | Age (y) | Sex | Eye | Preoperative | Postoperative[b] | Calculated Ablation (μm) | T1 | T2 |
| 1 | 57 | F | R | 0.52 | −0.18 | 113 | 1 | 108 |
| 1 | 65 | F | L | 0.70 | 0.10 | 100 | 12 | 12 |
| 2 | 32 | M | R | 0.22 | −0.08 | 100 | 3 | 108 |
| 2 | 32 | M | L | 0.15 | −0.08 | 110 | 3 | 108 |
| 3 | 57 | F | R | 0.52 | 0.05 | 114 | 24 | 96 |
| 3 | 57 | F | L | 1.22 | 0.15 | 120 | 3 | 96 |
| 4 | 66 | M | R | 0.70 | −0.08 | 120 | 12 | 18 |
| 4 | 66 | M | L | 0.70 | 0.22 | 121 | 12 | 18 |
| 5 | 61 | F | R | 0.52 | 0.15 | 140 | 6 | 18 |
| 5 | 61 | F | L | 0.52 | 0.10 | 125 | 3 | 18 |

BCVA = best-corrected visual acuity; F = female; L = left; logMAR = logarithm of minimal angle of resolution; M = male; R = right; T1 = mean time before achieving the best overall BCVA after surgery; T2 = follow-up period.

[a]Patients 2, 3, and 5 were blood relatives.

[b]Postoperative BCVA denotes the best overall BCVA after surgery.

genetically diagnosed as Thiel-Behnke corneal dystrophy between July 13, 2001 and May 14, 2010. Only the patients who were followed up for at least 12 months after the PTK surgery were enrolled in this study. The mean age of the patients was 55 ± 13 years (range: 32–66 years). None of the enrolled patients had any previous history of corneal surgery. The PTK surgery was performed for the patient's visual rehabilitation at the time when the patient complained of decreased vision or when the patient's best-corrected visual acuity (BCVA) had become worse than logMAR 0.15. Each of the 5 patients had experienced painful erosive episodes prior to undergoing the surgery. Three of the 5 patients were members of the same pedigree.

• MOLECULAR ANALYSIS: Peripheral blood samples were collected from all 5 patients after they had received a complete, detailed explanation of the study protocols. DNA was extracted from the peripheral blood lymphocytes using a commercially available kit (DNeasy Blood & Tissue Kit; QIAGEN GmbH, Hilden, Germany). Exons 4, 11, 12, and 13 of the *TGFBI* gene, as well as their flanking introns, were amplified by polymerase chain reaction (PCR) and directly sequenced on both strands using previously published primers.[27]

• INTERVENTIONAL PROCEDURE: PTK was performed by the use of 1 of 3 commercially available 193-nm excimer laser devices, each produced by a different company. Five eyes were treated using the EC-5000 excimer laser (NIDEK Co Ltd, Gamagori, Japan), 3 eyes were treated using the VISX S4IR excimer laser (Abbott Medical Optics Inc, Abbot Park, Illinois, USA), and the remaining 2 eyes were treated using the Technolas T-217z Zyoptix laser system (Bausch & Lomb, Rochester, New York, USA). In all 10 eyes, the epithelium was removed directly by the excimer laser, and the ablation continued

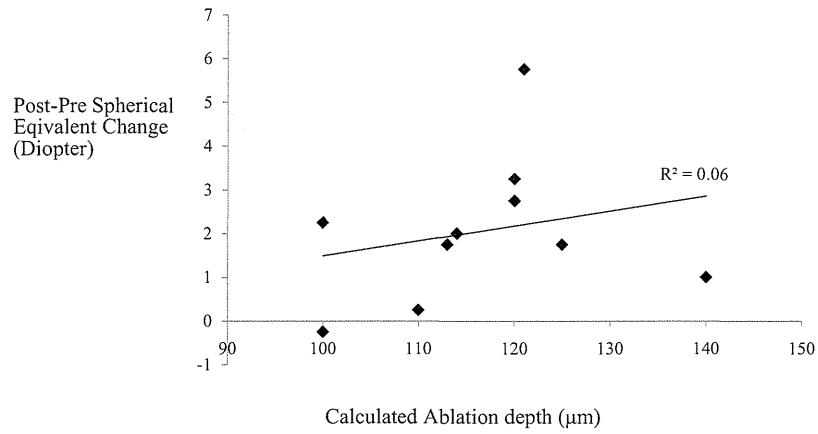


**FIGURE 2. A scattergram demonstrating the relationship between the spherical equivalent changes (between preoperative and postoperative) and the calculated ablation depth of phototherapeutic keratectomy surgery in eyes with Thiel-Behnke corneal dystrophy. Although the spherical equivalent change seems to have a tendency to increase with the increase of ablation depth, no statistically significant ($R^2 = 0.06$) association was found between the spherical equivalent changes and the calculated ablation depth.**

into the corneal stroma until approximately 50 μm of the stromal ablation was performed. During the surgery, the cornea of each eye was examined by use of the microscope equipped in the excimer laser devices under sclerotic scattering illumination using a vitrectomy-endoilluminator placed on the limbus.[28] When deemed necessary, additional ablations were performed to remove the bulk of the pathologic opacity from the visual axis. For all 10 eyes, the ablation was performed until the majority of opacities were removed, thus resulting in a mean calculated total ablation depth (including epithelium and stroma) of 116 ± 12 μm (range: 100–140 μm). Masking fluid was not used. Postoperatively, all 5 patients were initially administrated 0.1% fluorometholone (FLUMETHOLON; Santen Pharmaceutical Co, Ltd, Osaka, Japan) and 1.5% levofloxacin hydrate (CRAVIT; Santen Pharmaceutical Co, Ltd) 4 times daily, with a tapering-off of the dosage over 12 weeks. Each patient was instructed to continually wear a soft contact lens on the operated cornea until the epithelial defect had closed.

• MAIN OUTCOME MEASURES: In this present study, main outcome measures including BCVA, uncorrected visual acuity (UCVA), spherical equivalent (SE), and recurrence of Thiel-Behnke corneal dystrophy were assessed.

• CLINICAL DEFINITION FOR RECURRENCE OF THIEL-BEHNKE CORNEAL DYSTORPHY POST-PHOTOTHERAPEUTIC KERATECTOMY: The recurrence of Thiel-Behnke corneal dystrophy was considered significant when slit-lamp examination showed signs of increased central opacification of the superficial cornea that were also associated with significant visual loss (a 2-line or more loss of BCVA) according to the previous study.[15] The probability of recurrence of Thiel-Behnke corneal dystrophy after PTK surgery was calculated using the Kaplan-Meier method for survival analysis.[12,14,15,17]

• STATISTICAL ANALYSIS: For analysis of the results, Excel Tokei 2002 statistics software (SSRI Co Ltd, Tokyo, Japan) was used. Differences between paired samples were analyzed with the paired *t* test. A probability value of $<.05$ was considered statistically significant.

## RESULTS

THE P.ARG555GLN MUTATION WAS FOUND WITHIN THE *TGFBI* gene in all 5 patients. In all 5 patients, the superficial corneal opacities were successfully removed from the corneal visual axis (Figure 1). In all 10 eyes, epithelial defects closed within 3 to 5 days and visual acuity gradually improved in 3 to 24 months after the surgery (Table.). The mean follow-up period was 60 ± 46 months (range: 12–108 months). Postoperatively, all 5 patients requested to have PTK surgery performed to their contralateral eyes, thus indicating that they were satisfied with the results of the initial PTK surgery.

A 2-line or more increase in BCVA was found in all of the 10 enrolled eyes after the PTK surgery. The mean logMAR BCVA improved from 0.57 ± 0.29 preoperatively to the overall best of 0.04 ± 0.13 postoperatively, which was statistically significant ($P < .001$). The mean UCVA also significantly improved, from logMAR 0.84 ± 0.34 preoperatively to the overall best of logMAR 0.30 ± 0.26 postoperatively ($P < .01$). The average logMAR UCVA change was −0.54 ± 0.31.

The mean SE significantly increased from −1.63 ± 2.74 diopters (D) preoperatively to 0.43 ± 2.13 D postoperatively, which was statistically significant ($P < .01$). The

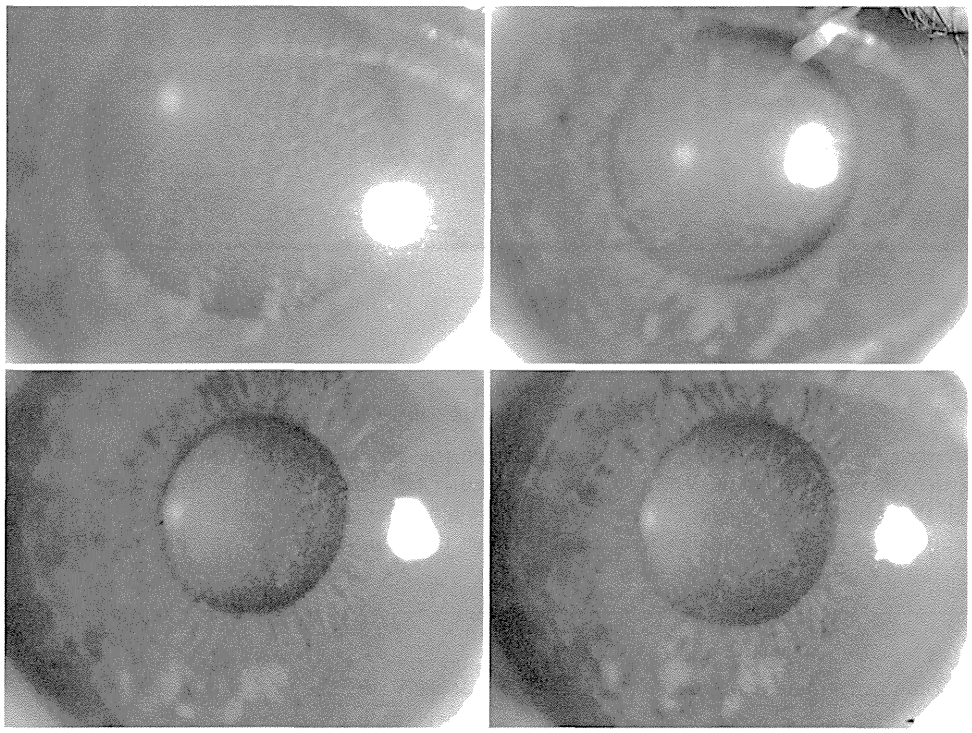

FIGURE 3. Slit-lamp microscopy images of the right eye of 32-year-old man with Thiel-Behnke corneal dystrophy (Patient 2) (Top left) before phototherapeutic keratectomy, (Top right), 3 years after phototherapeutic keratectomy, (Bottom left) 5 years after phototherapeutic keratectomy, and (Bottom right) 8.5 years after phototherapeutic keratectomy. The degree of the opacification at the final follow-up visit (Bottom right) is almost the same as that at 3 years after the phototherapeutic keratectomy surgery (Top right).

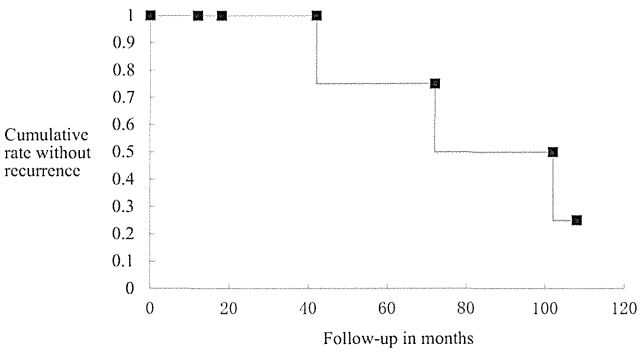


FIGURE 4. Line chart demonstrating the cumulative survival rate for the recurrence of Thiel-Behnke corneal dystrophy after phototherapeutic keratectomy analyzed by Kaplan-Meier survival analysis. The recurrence of Thiel-Behnke corneal dystrophy was defined by significant visual decrease with a 2-line or more loss of best-corrected visual acuity (BCVA) caused by the increased corneal opacification resulting from Thiel-Behnke corneal dystrophy.

average refractive change was +2.05 ± 1.68 D (range: −0.25 to +5.75 D). There was no apparent difference in the SE changes in relation to the type of excimer laser device used or to the calculated ablation depths (Figure 2).

Postoperative complications such as infection, delay in epithelial healing, or stromal haze were not noticed in any of the 10 eyes, and none of the patients experienced any postoperative painful erosive episode. During the follow-up period, 5 of the 10 eyes experienced recurrence of the central superficial opacification. One of those 5 eyes (the right eye of Patient 2) had only a 1-line decrease of visual acuity at 108 months postoperatively (Figure 3). However, in 4 of those 5 eyes, the degree of recurrence was significant enough to lead to a decrease in visual acuity of more than 2 lines, yet none of those patients requested a PTK reoperation at their final follow-up visit. The earliest significant recurrence (the right eye of Patient 3) was observed after 42 months (Figures 4 and 5). The remaining 5 of the 10 eyes exhibited no apparent signs of recurrence, possibly because the follow-up period for those eyes was not very long.

## DISCUSSION

IN THE PRESENT STUDY, PTK SURGERY FOR THIEL-BEHNKE corneal dystrophy was found to result in the significant midterm improvement of visual acuity for all patients. During the follow-up period, a gradual recurrence of central superficial opacification was observed, yet the level of the opacification was not severe enough to lead to a significant decrease in visual acuity for at least 42 months after surgery.

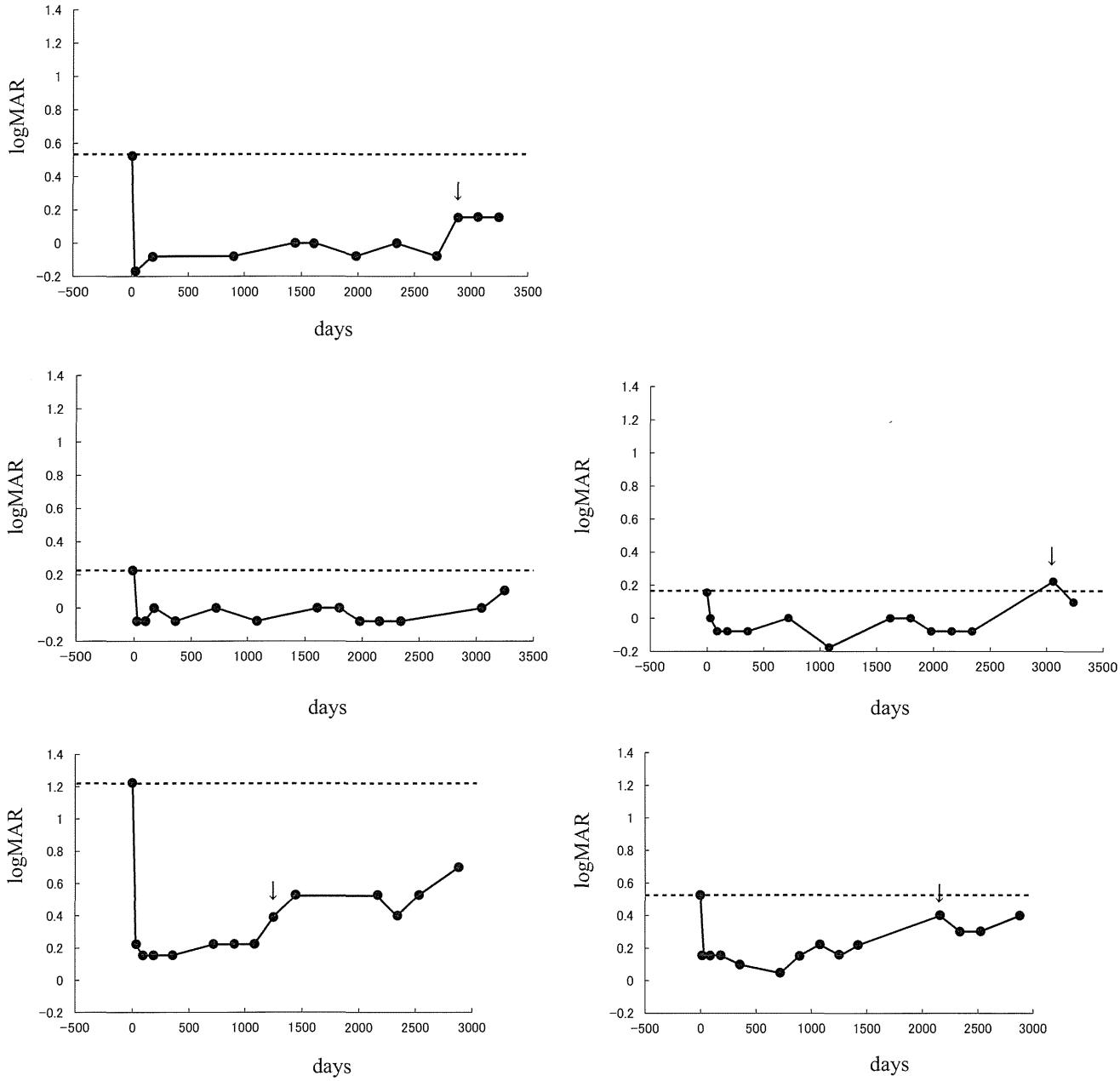


FIGURE 5. Polygonal line graphs denoting the time course of logMAR best-corrected visual acuity (BCVA) in 5 eyes of 3 Thiel-Behnke corneal dystrophy patients followed up for over 96 months after phototherapeutic keratectomy surgery. (Top) Right eye of a 57-year-old woman (Patient 1). (Middle left) Right eye of a 32-year-old man (Patient 2). (Middle right) Left eye of a 32-year-old man (Patient 2). (Bottom left) Right eye of a 57-year-old woman (Patient 3). (Bottom right) Left eye of a 57-year-old woman (Patient 3). Solid circles indicate the time points of the patients' follow-up visits. Arrows indicate the time points when significant recurrences were observed. Broken lines indicate the preoperative logMAR best-corrected visual acuity (BCVA). The recurrence of Thiel-Behnke corneal dystrophy was defined by significant visual decrease with a 2-line or more loss of BCVA caused by increased corneal opacification resulting from Thiel-Behnke corneal dystrophy. logMAR = logarithm of minimal angle of resolution.

To date, 3 previous studies have reported a successful clinical outcome in Thiel-Behnke corneal dystrophy patients after undergoing PTK surgery. The first study enrolled 6 eyes of 5 patients who were diagnosed with Thiel-Behnke corneal dystrophy just from the clinical appearance of their corneas and not by genetic analysis.[9] The second study enrolled 8 eyes of 4 patients who were clinically diagnosed with Thiel-Behnke corneal dystrophy but who had a genomic linkage to chromosome 10, which is therefore thought to be a distinct pathologic entity of the typical Thiel-Behnke corneal dystrophy bearing the p.Arg555Gln mutation within the *TGFBI* gene.[11] The third study enrolled 1 eye of 1 patient who had the p.Arg555Gln mutation within the *TGFBI* gene and who

underwent the PTK procedure on a grafted cornea that had undergone PKP.[12]

Reis-Bücklers corneal dystrophy[29] is a bilateral and autosomal dominant inheritable disease. This disease is clinically characterized by corneal opacities in a "geographic" pattern at the level of the Bowman layer, frequently associated with the episode of recurrent painful corneal erosion,[2] and has been referred to as corneal dystrophy of the Bowman layer and the superficial stroma type I (CDB1, OMIM#60847).[3] Because of the similarity of opacity pattern and opacity depth observed in Thiel-Behnke corneal dystrophy and Reis-Bücklers corneal dystrophy, considerable clinical confusion may still exist in distinguishing between these 2 diseases. Although the opacity pattern of Thiel-Behnke corneal dystrophy is reported to be apparently different from that of Reis-Bücklers corneal dystrophy, the opacity patterns of the 2 corneal dystrophies can appear to ordinary ophthalmologists to be quite similar, thus possibly resulting in considerable clinical confusion in discriminating between these 2 dystrophies. In the 1980s, Thiel-Behnke corneal dystrophy was considered to be a special type of Reis-Bücklers corneal dystrophy. These 2 corneal dystrophies of the Bowman layer were reported to be distinguishable through electron microscopy examination of the patient's corneal tissue. However, since a patient's corneal tissue is normally unavailable, it is often difficult to distinguish between these 2 dystrophies.[30] The only clinically identifiable difference between Thiel-Behnke corneal dystrophy and Reis-Bücklers corneal dystrophy is that Reis-Bücklers corneal dystrophy is clinically characterized by disease onset occurring in the patient at a younger age, the severe degree of corneal opacity, and a worse deterioration of vision compared to Thiel-Behnke corneal dystrophy.[2–4] Recent molecular biological analysis has revealed that Reis-Bücklers corneal dystrophy is caused by a mutation (p.Arg124Leu)[7] of the *TGFBI* gene that is distinct from that in Thiel-Behnke corneal dystrophy.

It should be noted that the early reports[19,20] of PTK for Reis-Bücklers corneal dystrophy possibly included Thiel-Behnke corneal dystrophy cases. In general, there is almost always a recurrence of Reis-Bücklers corneal dystrophy after PTK,[15] and even after PKP,[8] and the recurrence occurs earlier and with a more severe degree of disease compared with other *TGFBI*-related corneal dystrophies. However, despite the prominent similarities in several clinical attributes found in Thiel-Behnke corneal dystrophy and Reis-Bücklers corneal dystrophy, Thiel-Behnke corneal dystrophy patients demonstrated a relatively slow postoperative rate of recurrence after undergoing PTK surgery, as is shown in the findings of this present study. This finding may be the result of the difference in the molecular character of the TGFBI proteins that reflect each distinct mutation site. Thus, the simple PTK procedure appears to be an insufficient treatment for Reis-Bücklers corneal dystrophy. In a previous clinical trial, the usefulness of a topical administration of mitomycin C was assessed in Reis-Bücklers corneal dystrophy patients, and it was found to have a beneficial effect on preventing recurrence after PTK surgery.[31] Thus, it is very important to perform gene mutation analysis against the *TGBFI* gene to definitively discriminate Thiel-Behnke corneal dystrophy from Reis-Bücklers corneal dystrophy in order to make a more precise prediction of postoperative prognosis, as well as to consider the possible additional treatments, such as the administration of mitomycin C, that will be needed when patients are diagnosed as having Reis-Bücklers corneal dystrophy.

In conclusion, the findings of the present study show that PTK is a successful therapy for Thiel-Behnke corneal dystrophy. It should be noted that this study was retrospective and that the sample size was not very large. In addition, *TGFBI* corneal dystrophies sometimes demonstrate varying degrees of severity even with the same gene mutation. Thus, it is difficult to make a generalized statement as to the efficacy of PTK surgery for Thiel-Behnke corneal dystrophies from the limited results presented in this study. However, and to the best of our knowledge, this is the first report to demonstrate the midterm clinical outcome of PTK surgery for Thiel-Behnke corneal dystrophy patients who were diagnosed strictly by gene mutation analysis to have the p.Arg555Gln mutation and who had not undergone any surgery to their corneas prior to the PTK surgery. We hope that a randomized controlled trial will be conducted in the future in order to better understand the more precise clinical course of Thiel-Behnke corneal dystrophy after PTK surgery.

ALL AUTHORS HAVE COMPLETED AND SUBMITTED THE ICMJE FORM FOR DISCLOSURE OF POTENTIAL CONFLICTS OF Interest. Sa.K. and Sh.K. indicate receipt of grant support. Supported by a grant-in aid (#21592238) for scientific study from the Japanese Ministry of Education, Science, Culture and Sports and by a grant (H23-Nanchi-Ippan-084) from the Japanese Ministry of Health, Labor and Welfare, and research fund from the Kyoto Foundation for the Promotion of Medical Science (Kyoto, Japan). Involved in design of the study (O.H., Sa.K.); conduct of the study (O.H., Sh.K.); collection, management, analysis, and interpretation of the data (O.H., K.W., K.Y., T.I.); and preparation, review (O.H., Sa.K.), and approval of the manuscript (O.H., Sa.K., K.W., K.Y., T.I., Sh.K.). This retrospective review of patient data was approved by the Human Studies Committee of Kyoto Prefectural University of Medicine, and all patients gave informed consent to participate in further research by providing blood samples for mutation analysis under a defined IRB-approved protocol.

The authors wish to thank Mr John Bush for reviewing the manuscript, and Shounosuke Okamoto (Okamoto Eye Clinic) and Ichirou Watanabe (Kawasaki Medical University) for the data collection.

## REFERENCES


1. Thiel HJ, Behnke H. [A hitherto unknown subepithelial hereditary corneal dystrophy]. *Klin Monbl Augenheilkd* 1967; 150(6):862–874.
2. Weiss JS, Moller HU, Lisch W, et al. The IC3D classification of the corneal dystrophies. *Cornea* 2008;27(Suppl 2):S1–83.
3. Küchle M, Green WR, Volcker HE, Barraquer J. Reevaluation of corneal dystrophies of Bowman's layer and the anterior stroma (Reis-Bücklers and Thiel-Behnke types): a light and electron microscopic study of eight corneas and a review of the literature. *Cornea* 1995;14(4):333–354.
4. Mashima Y, Yamada M, Oguchi Y. [Autosomal dominant inherited corneal dystrophies associated with TGFBI mutation]. *Nippon Ganka Gakkai Zasshi* 2001;105(10):659–672.
5. Munier FL, Frueh BE, Othenin-Girard P, et al. BIGH3 mutation spectrum in corneal dystrophies. *Invest Ophthalmol Vis Sci* 2002;43(4):949–954.
6. Munier FL, Korvatska E, Djemai A, et al. Kerato-epithelin mutations in four 5q31-linked corneal dystrophies. *Nat Genet* 1997;15(3):247–251.
7. Okada M, Yamamoto S, Tsujikawa M, et al. Two distinct kerato-epithelin mutations in Reis-Bucklers corneal dystrophy. *Am J Ophthalmol* 1998;126(4):535–542.
8. Ellies P, Renard G, Valleix S, Boelle PY, Dighiero P. Clinical outcome of eight BIGH3-linked corneal dystrophies. *Ophthalmology* 2002;109(4):793–797.
9. Amm M. [Photo-therapeutic keratectomy (PTK)—a successful treatment for Thiel-Behnke dystrophy and its recurrence]. *Ophthalmologe* 1999;96(8):489–493.
10. Fagerholm P. Phototherapeutic keratectomy: 12 years of experience. *Acta Ophthalmol Scand* 2003;81(1):19–32.
11. Sorour HM, Yee SB, Peterson NJ, et al. Recurrence of chromosome 10 Thiel-Behnke corneal dystrophy (CDB2) after excimer laser phototherapeutic keratectomy or penetrating keratoplasty. *Cornea* 2005;24(1):45–50.
12. Ellies P, Bejjani RA, Bourges JL, Boelle PY, Renard G, Dighiero P. Phototherapeutic keratectomy for BIGH3-linked corneal dystrophy recurring after penetrating keratoplasty. *Ophthalmology* 2003;110(6):1119–1125.
13. Paparo LG, Rapuano CJ, Raber IM, Grewal S, Cohen EJ, Laibson PR. Phototherapeutic keratectomy for Schnyder's crystalline corneal dystrophy. *Cornea* 2000;19(3):343–347.
14. Hafner A, Langenbucher A, Seitz B. Long-term results of phototherapeutic keratectomy with 193-nm excimer laser for macular corneal dystrophy. *Am J Ophthalmol* 2005;140(3): 392–396.
15. Dinh R, Rapuano CJ, Cohen EJ, Laibson PR. Recurrence of corneal dystrophy after excimer laser phototherapeutic keratectomy. *Ophthalmology* 1999;106(8):1490–1497.
16. Das S, Langenbucher A, Seitz B. Delayed healing of corneal epithelium after phototherapeutic keratectomy for lattice dystrophy. *Cornea* 2005;24(3):283–287.
17. Pogorelov P, Langenbucher A, Kruse F, Seitz B. Long-term results of phototherapeutic keratectomy for corneal map-dot-fingerprint dystrophy (Cogan-Guerry). *Cornea* 2006;25(7): 774–777.
18. O'Brart DP, Gartry DS, Lohmann CP, Patmore AL, Kerr Muir MG, Marshall J. Treatment of band keratopathy by excimer laser phototherapeutic keratectomy: surgical techniques and long term follow up. *Br J Ophthalmol* 1993;77(11): 702–708.
19. Hahn TW, Sah WJ, Kim JH. Phototherapeutic keratectomy in nine eyes with superficial corneal diseases. *Refract Corneal Surg* 1993;9(2 Suppl):S115–118.
20. Hersh PS, Spinak A, Garrana R, Mayers M. Phototherapeutic keratectomy: strategies and results in 12 eyes. *Refract Corneal Surg* 1993;9(2 Suppl):S90–95.
21. Kozobolis VP, Siganos DS, Meladakis GS, Pallikaris IG. Excimer laser phototherapeutic keratectomy for corneal opacities and recurrent erosion. *J Refract Surg* 1996;12(2): S288–290.
22. John ME, Van der Karr MA, Noblitt RL, Boleyn KL. Excimer laser phototherapeutic keratectomy for treatment of recurrent corneal erosion. *J Cataract Refract Surg* 1994;20(2): 179–181.
23. Marcon AS, Rapuano CJ. Excimer laser phototherapeutic keratectomy retreatment of anterior basement membrane dystrophy and Salzmann's nodular degeneration with topical mitomycin C. *Cornea* 2002;21(8):828–830.
24. Thomann U, Meier-Gibbons F, Schipper I. Phototherapeutic keratectomy for bullous keratopathy. *Br J Ophthalmol* 1995; 79(4):335–338.
25. Sharma N, Prakash G, Sinha R, Tandon R, Titiyal JS, Vajpayee RB. Indications and outcomes of phototherapeutic keratectomy in the developing world. *Cornea* 2008;27(1): 44–49.
26. Fujita A, Hieda O, Nakajima N, Kinoshita S. [The VF-14 index of functional visual impairment in patients with corneal disease treated by phototherapeutic keratectomy]. *Nihon Ganka Gakkai Zasshi* 2005;109(11):736–740.
27. Fukuoka H, Kawasaki S, Yamasaki K, et al. Lattice corneal dystrophy type IV (p.Leu527Arg) is caused by a founder mutation of the TGFBI gene in a single Japanese ancestor. *Invest Ophthalmol Vis Sci* 2010;51(9):4523–4530.
28. Hayashi H, Maeda N, Ikeda Y, Nishida K, Watanabe H, Tano Y. Sclerotic scattering illumination during phototherapeutic keratectomy for better visualization of corneal opacities. *Am J Ophthalmol* 2003;135(4):559–561.
29. Bücklers M. Uber eine weitere familiäre Hornhaut-dystrophie (Reis). *Klin Monatsbl Augenkeilkd* 1949;114:386–397.
30. Kobayashi A, Sugiyama K. In vivo laser confocal microscopy findings for Bowman's layer dystrophies (Thiel-Behnke and Reis-Bücklers corneal dystrophies). *Ophthalmology* 2007; 114(1):69–75.
31. Miller A, Solomon R, Bloom A, Palmer C, Perry HD, Donnenfeld ED. Prevention of recurrent Reis-Bücklers dystrophy following excimer laser phototherapeutic keratectomy with topical mitomycin C. *Cornea* 2004;23(7):732–735.

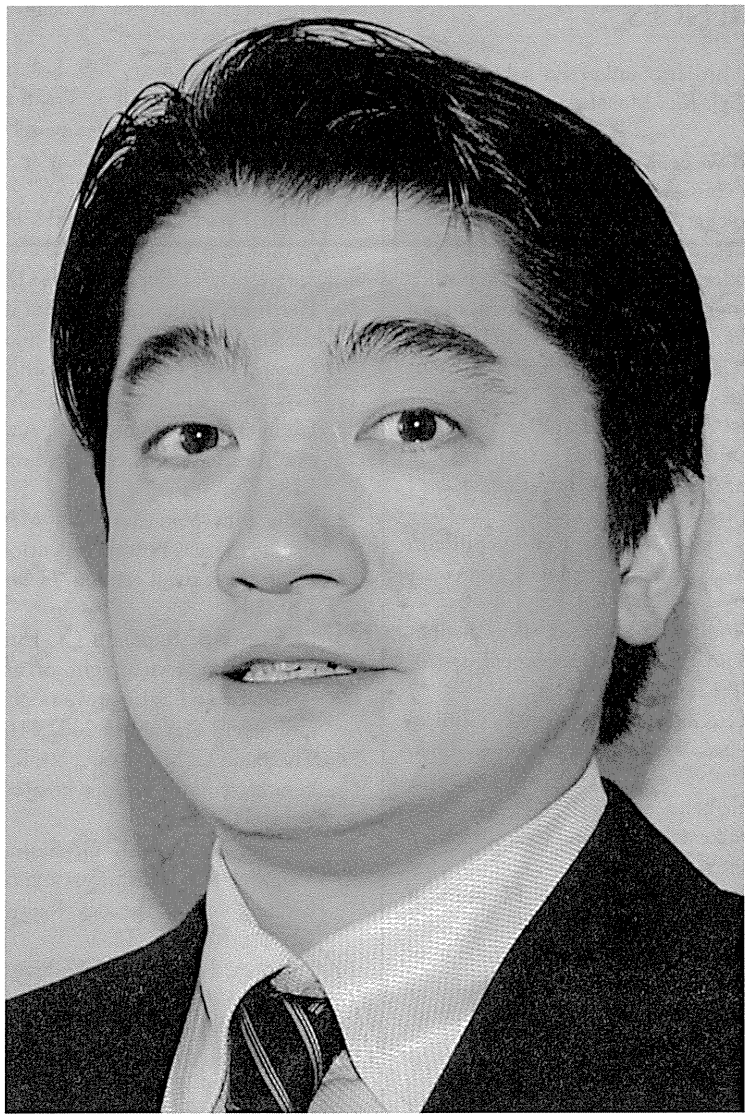

## Biosketch

Osamu Hieda, MD, is a staff doctor at the Department of Ophthalmology, Kyoto Prefectural University of Medicine, Kyoto, Japan, where he received his clinical training and corneal refractive surgery fellowship. Dr Hieda's current interests include laser surgery for the treatment of corneal dystrophies.

# Epithelial-Mesenchymal Transition-Like Phenotypic Changes of Retinal Pigment Epithelium Induced by TGF-β Are Prevented by PPAR-γ Agonists

*Hiroki Hatanaka,*[1] *Noriko Koizumi,*[2] *Naoki Okumura,*[1,2] *EunDuck P. Kay,*[2,3] *Eri Mizuhara,*[2] *Junji Hamuro,*[1] *and Shigeru Kinoshita*[1]

**Purpose.** Proliferative eye diseases, such as proliferative vitreoretinopathy and proliferative diabetic retinopathy, are caused partly by fibrotic change of retinal pigment epithelial cells (RPECs). The purpose of our study was to examine the effect of the peroxisome proliferator-activated receptor-γ (PPAR-γ) agonist on the fibrotic change of primate RPECs.

**Methods.** Monkey RPECs (MRPECs) isolated from a cynomolgus monkey eye were subcultured. To induce fibrotic change, MRPECs were cultured with TGF-β2 (3 ng/mL), and also cultured in the coexistence of TGF-β2 and the PPAR-γ agonist pioglitazone (30 μM). The phenotype of the cultured MRPECs was evaluated by phase contrast microscopy and immunocytochemical analysis. The phosphorylation of Smad2/Smad3 proteins was examined by Western blot analysis.

**Results.** Primary MRPECs were cultured as a monolayer with a hexagonal cell shape, and positive expression of ZO-1, $Na^+/K^+$-ATPase, and RPE65 was confirmed. Cell morphology and the expression of these markers were maintained in the presence of pioglitazone, whereas the cells were elongated and the expression of these markers was reduced in its absence. Conversely, the expression of phalloidin, α-smooth muscle actin, and fibronectin was reduced in the presence of pioglitazone, whereas it was increased in the absence. Western blot assay demonstrated that phosphorylation of Smad2/Smad3 proteins was suppressed by pioglitazone.

**Conclusions.** The PPAR-γ agonist pioglitazone inhibited the fibrotic change of primary MRPECs through the suppression of TGF-β signaling. Pioglitazone might prove to be a clinically applicable and effective pharmaceutic treatment for proliferative eye diseases. (*Invest Ophthalmol Vis Sci.* 2012;53:6955–6963) DOI:10.1167/iovs.12-10488

Intraocular proliferative diseases, such as proliferative vitreoretinopathy (PVR) and proliferative diabetic retinopathy (PDR), are the major cause of vision loss and have poor visual prognosis in spite of the development of innovative surgical techniques and anti-VEGF agents.[1,2] Despite the vigorous accumulation of knowledge about the pathology of PVR over the past decade, little progress has been made toward the clinical management of the disease.[2] To date, to our knowledge no practical pharmacologic treatment has been developed to repair the damaged fibrotic tissues involved in these diseases.

Intraocular fibrosis is a clinically-recognized, underlying pathologic feature in PVR and PDR that leads to functional impairment of the retina. The fibrotic change involves sub- and preretinal fibrosis, scarring, and proliferative membrane. These fibrotic features result in the recurrence of the disease and aggravate the prognosis of visual acuity.[3,4] Such tissue fibrosis also is found in a variety of tissues, such as those of the kidney, liver, lung, and so forth. The fibrous tissue reduces the flexibility of the detached retina and becomes a major cause for failure of retinal reattachment surgery. Once fibrosis occurs, a surgical operation thus far has been the only possible therapeutic modality. In the pathogenesis of PVR and PDR, changes such as proliferation and production of the fibrillar extracellular matrix (ECM) on the retina, occur frequently in retinal pigment epithelial cells (RPECs) located in the vitreous cavity and subretinal space.[2,5] Thus, agents capable of preventing the fibrotic change of RPECs may be of great therapeutic value in retinal reattachment surgery. Numerous drugs have been tested on animal models or cell cultures to inhibit cell proliferation and proliferative membrane formation. However, many of these drugs cause severe side effects and only a few have been used in clinical trials.[2,6]

The epithelial mesenchymal transition (EMT) or transdifferentiation of epithelial cells has been theorized to have a critical role in the development of such pathologic fibrosis.[7–10] In fact, TGF-β signaling has been shown to have a crucial role in these fibrotic changes.[11,12] Recently, numerous reports have demonstrated that treatment with a peroxisome proliferator-activated receptor-γ (PPAR-γ) agonist attenuates experimentally-induced kidney,[13,14] liver,[15] lung,[16] skin,[17] and cardiac fibrosis.[18] In a variety of renal diseases, overexpression of TGF-β isoforms is observed in animals and humans.[19–22] These reports also showed that the PPAR-γ agonist inhibited the fibrotic change by down-regulating the TGF-β pathway.

Likewise, the overexpression of TGF-β has been observed in the vitreous body in PDR and PVR,[23,24] and also has been investigated in relation to the proliferative membranes in these diseases.[25] The purpose of our study was to investigate if a human RPE cell line and primate RPECs exhibited fibrotic changes by TGF-β2, and if PPAR-γ agonists could prevent this fibrotic process. Our findings demonstrated that

From the [1]Department of Ophthalmology, Kyoto Prefectural University of Medicine, Kyoto, Japan; the [2]Department of Biomedical Engineering, Faculty of Life and Medical Sciences, Doshisha University, Kyotanabe, Japan; and the [3]University of Southern California, Los Angeles, California.

The authors alone are responsible for the content and writing of the paper.

Submitted for publication June 28, 2012; revised August 20 and August 31, 2012; accepted August 31, 2012.

Disclosure: **H. Hatanaka**, None; **N. Koizumi**, None; **N. Okumura**, None; **E.P. Kay**, None; **E. Mizuhara**, None; **J. Hamuro**, None; **S. Kinoshita**, None

Corresponding author: Noriko Koizumi, Department of Biomedical Engineering, Faculty of Life and Medical Sciences, Doshisha University, Kyotanabe 610-0321, Japan; nkoizumi@mail.doshisha.ac.jp.

the PPAR-γ agonist restored the fibrotic pathologic changes mediated by TGF-β2.

## METHODS

### Materials

For our study, recombinant human TGF-β2 was purchased from R&D Systems, Inc. (Minneapolis, MN). Pioglitazone was purchased from Enzo Life Sciences, Inc. (Farmingdale, NY). Dulbecco's modified Eagle medium:Nutrient Mixture (DMEM/F12), penicillin, streptomycin, Alexa Fluor 546 phalloidin, Alexa Fluor 488 donkey anti-mouse IgG, and Alexa Fluor 594 donkey anti-rabbit IgG were purchased from Life Technologies Corporation (Carlsbad, CA). Dispase II was purchased from Roche Applied Science (Penzberg, Germany), and FNC Coating Mix was purchased from Athena Environmental Sciences, Inc. (Baltimore, MD). ZO-1 polyclonal antibody was purchased from Zymed Laboratories, Inc. (South San Francisco, CA), $Na^+$-$K^+$-ATPase monoclonal antibody was purchased from Upstate Biotechnology, Inc. (Lake Placid, NY), and DAPI was purchased from Vector Laboratories, Inc. (Burlingame, CA). N-cadherin and fibronectin antibody were purchased from BD Biosciences Pharmingen (Franklin Lakes, NJ). Smad-2, Smad3, and phosphorylated Smad2 (phospho-Smad2) and phosphor-Smad3 antibody were purchased from Cell Signaling Technology, Inc. (Danvers, MA). Alpha smooth muscle (αSMA) antibody was purchased from Thermo Fisher Scientific, Inc. (Waltham, MA). RPE65 antibody and GAPDH were purchased from Abcam, Inc. (Cambridge, MA). Phosphatase inhibitor was purchased from Sigma-Aldrich Corporation (St. Louis, MO).

### Animal Experiment Approval

In all experiments, animals were housed and treated in accordance with the ARVO Statement for the Use of Animals in Ophthalmic and Vision Research.

### Cell Culture and Treatment of ARPE-19

ARPE-19, a human RPE cell line, was purchased from the American Type Culture Collection (ATCC; Manassas, VA). The cells were cultured in DMEM/F12 supplemented with 10% fetal bovine serum (FBS), 50 U/mL penicillin, and 50 μg/mL streptomycin in a humidified atmosphere at 37°C in 5% $CO_2$ for more expansion.[26] As described previously, the cells were treated in the fresh medium with recombinant human TGF-β2 (5 ng/mL, fibrotic group) or serum-free medium (control group) after 24 hours of serum starvation when the cells reached confluency.[27] Next, we investigated if a difference could be found between the control and fibrotic groups in the morphology of ARPE-19. The ratio of elongated cells cultured under various conditions then was calculated. The elongated cells were defined as ones in which the length of the cell is two times longer than the width of that cell. ARPE-19 cells were seeded at a density of $1.0 \times 10^5$ cells onto 12-well plates in the medium containing 10% FBS. PPAR-γ agonist was added at the concentration of 10 and 30 μM with TGF-β2 (PPAR-γ group) simultaneously.

### Cell Culture and Treatment of Monkey RPECs (MRPECs)

MRPECs were cultured from the posterior area of an eyeball enucleated from a cynomolgus monkey (3–5 years old, estimated equivalent human age 5–20 years) housed at Nissei Bilis Co., Ltd. (Otsu, Japan). The MRPECs then were separated from the RPEC fragments in accordance with the method described previously for human fetal RPE.[28] The MRPECs then were cultured on FNC Coating Mix-coated dishes in DMEM/F12 supplemented with 10% FBS, 50 U/mL of penicillin, and 50 μg/mL of streptomycin for more expansion in a humidified atmosphere at 37°C in 5% $CO_2$. The culture medium then was changed every 2 days. When the cells reached confluency in 5 to 7 days, they were rinsed in $Ca^{2+}$ and $Mg^{2+}$-free Dulbecco's phosphate-buffered saline (PBS), trypsinized with 0.05% Trypsin-EDTA (Life Technologies) for 5 minutes at 37°C, and passaged at ratios of 1:2 to 4. Cultivated MRPECs at passages 1 to 3 were used for all experiments. MRPECs then were treated with recombinant human TGF-β2 (3 ng/mL) (fibrotic group) or 2% FBS-containing medium (control) after 24 hours of serum starvation when the cells reached confluency. As a PPAR-γ group, MRPECs were cultured with medium containing TGF-β2 and PPAR-γ agonist (30 μM). The morphologic differences among the groups then were observed. The MRPECs then were seeded at a density of $1.0 \times 10^5$ cells onto 24-well plates in the medium containing 10% FBS to investigate if a difference in cell morphology could be found among the groups.

### Immunocytochemistry

To analyze the expression and localization of function-related proteins in the cells, ARPE-19 cells and MRPECs were cultured at a density of $3 \times 10^4$ cells/cm$^2$ on Lab-Tek Chamber Slides (NUNC A/S, Roskilde, Denmark) in various conditions for 48 hours before staining. The cells then were stained with individual antibodies; namely, anti-ZO-1, anti-$Na^+$/$K^+$-ATPase, anti-RPE65, anti-N cadherin, anti-E cadherin, anti-phalloidin, anti-fibronectin, and anti-α smooth muscle antibodies. For a second antibody, 1:2000 diluted Alexa Fluor 488 donkey anti-mouse IgG and 1:2000 diluted Alexa Fluor 594 donkey anti-rabbit IgG were used. Cell nuclei then were stained with DAPI, and the slides were inspected by use of a fluorescence microscope.

### Reverse Transcriptase-Polymerase Chain Reaction (RT-PCR)

For RT-PCR, total RNA was extracted by use of TRIzol reagent (Life Technologies) and treated with RNase-free DNase I (Roche). cDNA was synthesized with SuperScript III Reverse Transcriptase (Life Technologies) and PCR reactions then were performed with EX Taq DNA polymerase (Takara Bio, Shiga, Japen) as follows: denaturation at 94°C for 30 seconds, 23 to 35 cycles of annealing at 55°C to 57°C for 30 seconds, and elongation at 72°C for 30 seconds. The PCR products then were separated by electrophoresis on 2% agarose gels and detected under ultraviolet illumination.

### Real-Time Quantitative PCR (qPCR)

For the real-time qPCR, reverse transcription was conducted using the TaqMan Fast Advanced Master Mix (Applied Biosystems, Inc., Foster City, CA) according to the manufacturer's protocol. Real-time qPCR reactions then were conducted by use of the StepOnePlus (Applied Biosystems) real-time PCR system according to the manufacturer's protocol.

### Western Blot Analysis

For the detection of Smad2, Smad3, phospho-Smad2, and phospho-Smad3, MRPECs were serum-starved for 24 hours and then incubated with TGF-β2, or TGF-β2 and PPAR-γ agonist-containing medium for 10 minutes and extracted with Tris-buffered saline containing phosphatase inhibitors. The proteins then were separated by use of SDS-PAGE and transferred to a polyvinylidene fluoride membrane. The blots were blocked overnight with nonfat dried milk and incubated with rabbit anti-human phospho-Smad2 monoclonal antibody, rabbit anti-human phospho-Smad3 monoclonal antibody, rabbit anti-human Smad2, or rabbit anti-human Smad3. Luminescence was observed by use of an ImageQuant LAS-4000

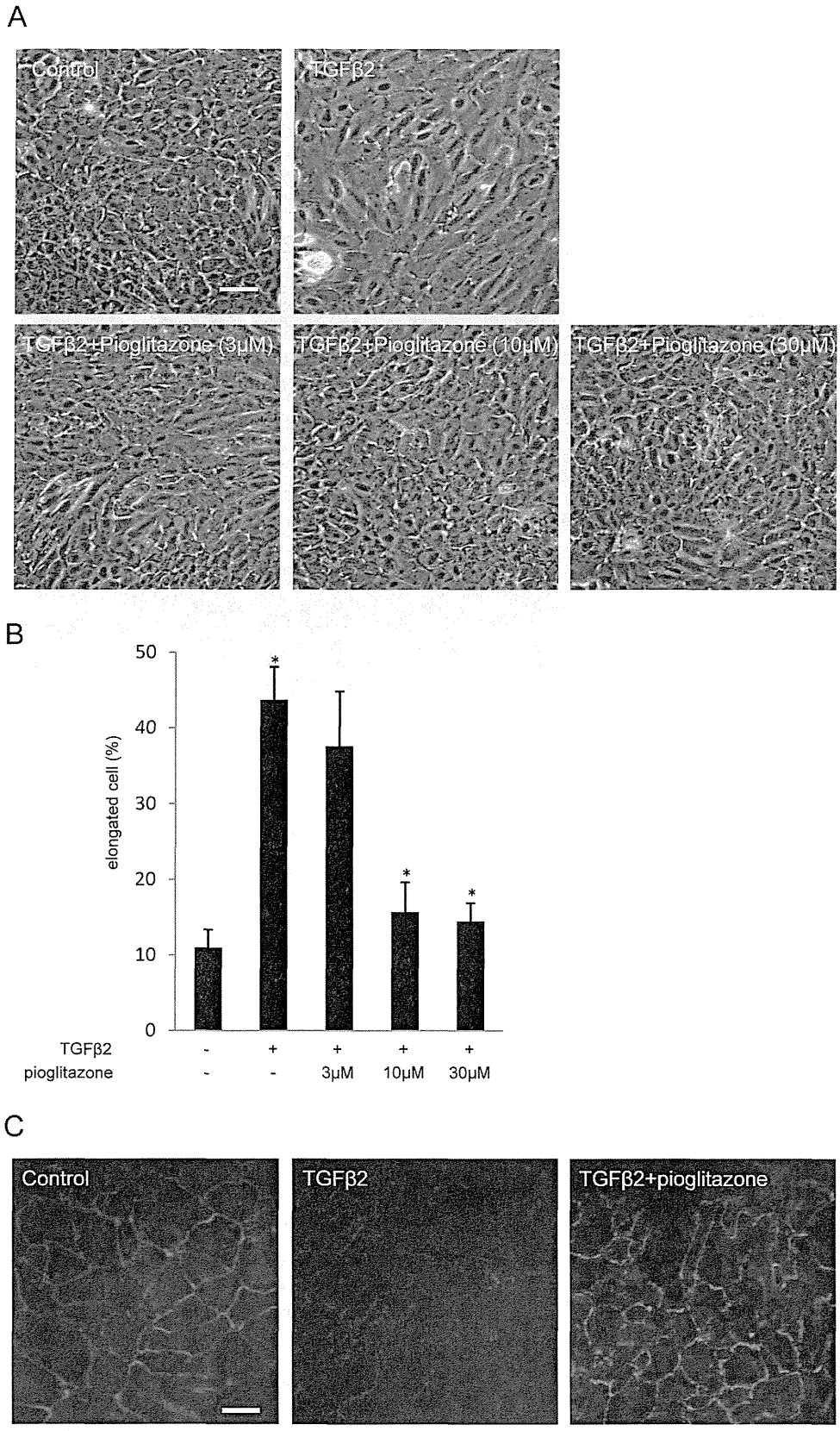


**Figure 1.** Fibrotic change induced by TGF-β2 and the inhibitory effect of pioglitazone on the morphologic change in ARPE-19 cells. Phase-contrast light microscope images of ARPE-19 cells with TGF-β2 (5 ng/mL) and pioglitazone (3, 10, 30 μM; [**A**]), the ratio of elongated cells in each condition (i.e., the control, TGFβ, and PPAR-γ conditions; [**B**]; $n = 4$; $P < 0.005$), and immunocytochemical staining of ZO-1 (**C**) are shown. *Scale bar*: 100 μm.

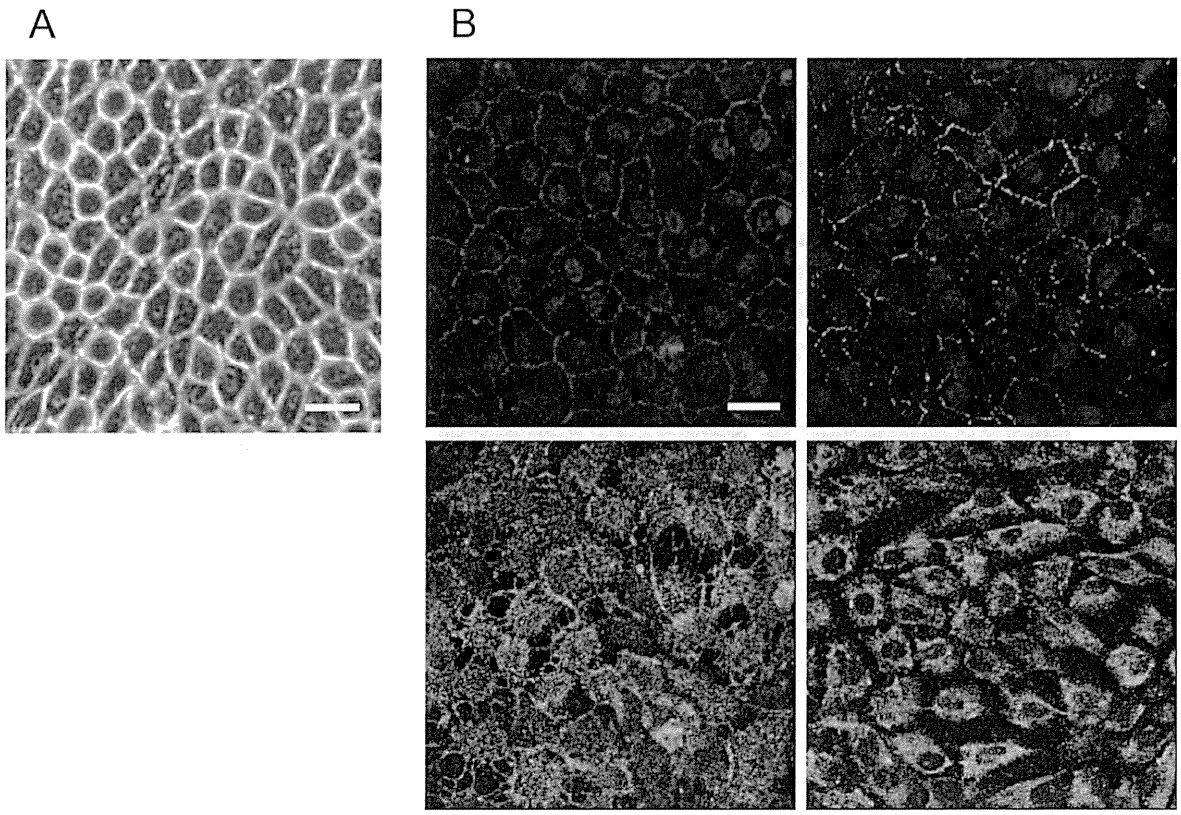


FIGURE 2. Images of primary MRPECs ($P = 1$) immunocytochemically stained (**A**) with ZO-1 (*top left*), N-cadherin (*top right, green*), $Na^+/K^+$-ATPase (*bottom left*), RPE65 (*bottom right, green*), and a phase-contrast light microscopy image (**B**). *Scale bar*: 100 μm.

mini (FUJIFILM, Tokyo, Japan) dedicated charge-coupled device (CCD) camera system.[29]

## RESULTS

### Preventive Effect of PPAR-γ Agonist against the TGF-β2–Induced Morphologic Change in ARPE-19

The cellular morphology of ARPE-19 cells is the characteristic cuboidal shape under normal culture conditions. On the other hand, the presence of TGF-β2 (5 ng/mL) induced an EMT-like morphologic change of ARPE-19 cells, symbolized by the elongated and fibroblastic phenotypes (Fig. 1A). TGF-β2 at 5 ng/mL, a concentration that is nontoxic and is known to be the most effective, was used in the following experiments. When cells were treated simultaneously with TGF-β2 and PPAR-γ agonist (pioglitazone), pioglitazone at 3 μM demonstrated a mixture of cuboidal and elongated cell shapes, while pioglitazone at 10 and 30 μM reversed the fibroblastic cell shape mediated by TGF-β2 to the cuboidal cell shape. Those results indicated that the PPAR-γ agonist has a concentration-dependent preventive effect against the fibrotic or EMT-like phenotypic change of ARPE-19 cells induced by TGF-β2 (Fig. 1B). The preventive effect of pioglitazone toward the TGF-β2-mediated phenotypic changes of ARPE-19 was confirmed further by use of ZO-1, one of the major epithelial functional tight junction molecules. The immunostaining of ARPE-19 cells with ZO-1 antibody showed the characteristic staining pattern of ZO-1 at the plasma membrane, while cells treated with TGF-β2 greatly reduced the ZO-1 staining potential. On the other hand, cells treated with TGF-β2 and pioglitazone demonstrated the cuboidal cell shape with the distinct ZO-1 staining pattern (Fig. 1C).

### Influence of PPAR-γ Agonist and TGF-β2 on the Expression of Functional Molecules in MRPECs

The established MRPEC cultures were maintained in DMEM/F12 medium containing 2% FBS, a concentration that minimizes the TGF-β activity of FBS, and the MRPECs demonstrated the characteristic hexagonal or polygonal morphology (Fig. 2A). That culture condition also maintained the expression of functional proteins, such as ZO-1, $Na^+/K^+$-ATPase, N-cadherin, and RPE65 (an essential protein for the visual cycle), and the proteins were expressed according to their subcellular localization (Fig. 2B).

When MRPECs were treated with TGF-β2, they lost their characteristic polygonal cell morphology. However, simultaneous treatment of the cells with TGF-β2 and pioglitazone reversed the cell shape change induced by TGF-β2 (Fig. 3A). Those results indicated the induction of the EMT-like or fibrotic change of MRPECs by TGF-β2 (Fig. 3A). TGF-β2 (3 ng/mL) was chosen as the optimal concentration for the induction of the fibrotic change of the MRPECs. The morphologic changes of the MRPECs induced by TGF-β2 (the EMT-like or fibrotic change) were reduced in the presence of pioglitazone below those in the TGF-β2 group.

The changes of distribution of ZO-1 (Fig. 3B), $Na^+/K^+$-ATPase (Fig. 3C), and N-cadherin (Fig. 3D) in the MRPECs were observed in the TGF-β2–treated group when compared to those of control cells. However, the TGF-β2 changes were inhibited by the PPAR-γ agonist pioglitazone (Figs. 3B, 3C, 3D). The expression of RPE65 and N-cadherin was examined further by use of real-time qPCR, which showed that the RPE65 expression was reduced markedly by TGF-β2, while the N-cadherin mRNA was increased by TGF-β2. Of interest, pioglitazone blocked such TGF-β2–mediated changes (Fig. 3E). The same tendency was observed in N-cadherin mRNA expressions using real-time PCR (Fig. 3F).

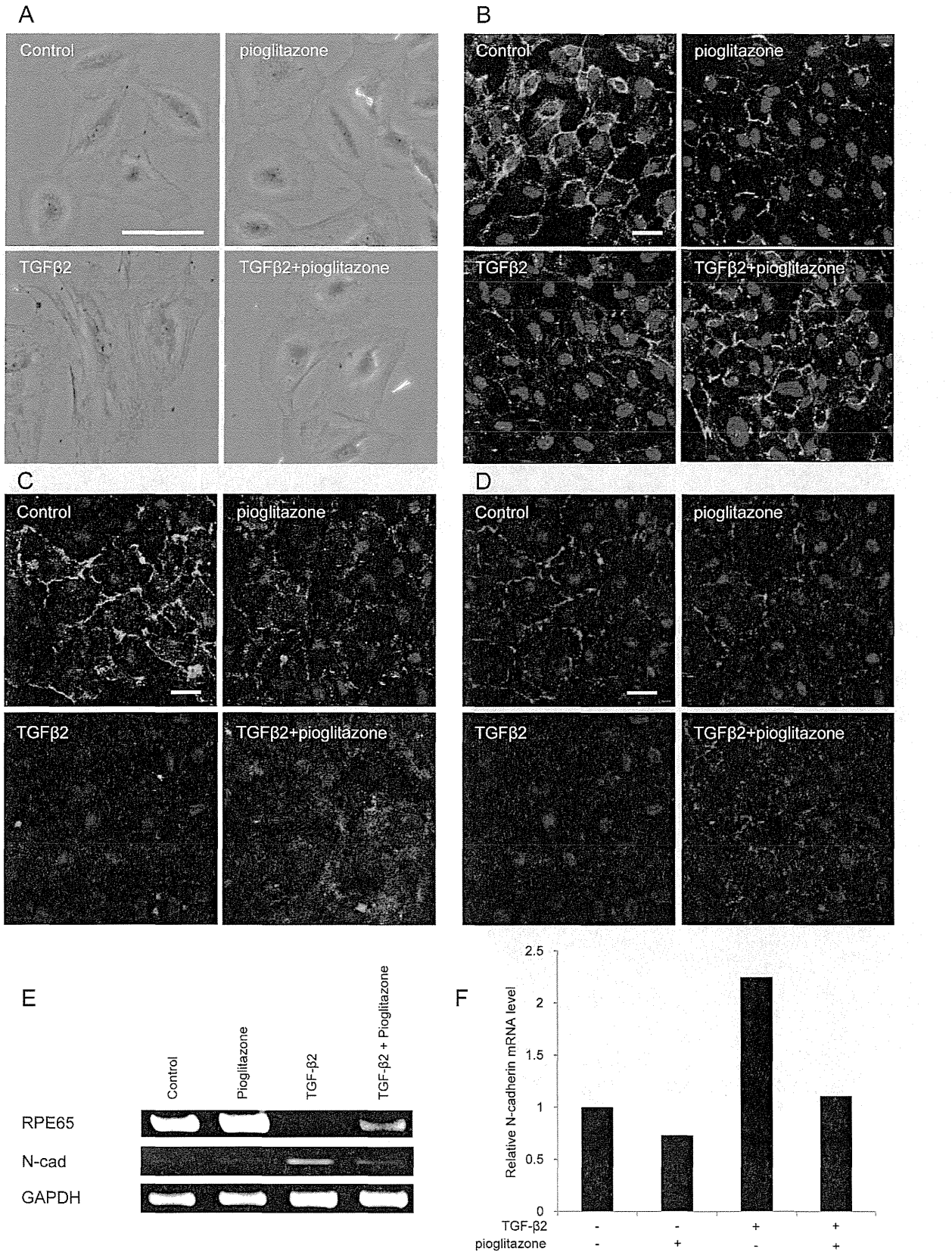


**Figure 3.** The effect of pioglitazone on fibrotic change induced by TGF-β2 in primary MRPECs. Phase-contrast light microscopy images of primary MRPECs (**A**), and the change of distribution in the expression of N-cadherin (**B**), $Na^+/K^+$-ATPase (**C**), and ZO-1 (**D**) in the medium with TGF-β2 (3 ng/mL) and/or pioglitazone (30 μM). (**E**) An image showing the mRNA expression of RPE65 and N-cadherin. (**F**) An image showing the ratio of the expression of N-cadherin mRNA as compared to the control. *Scale bar*: 100 μm.

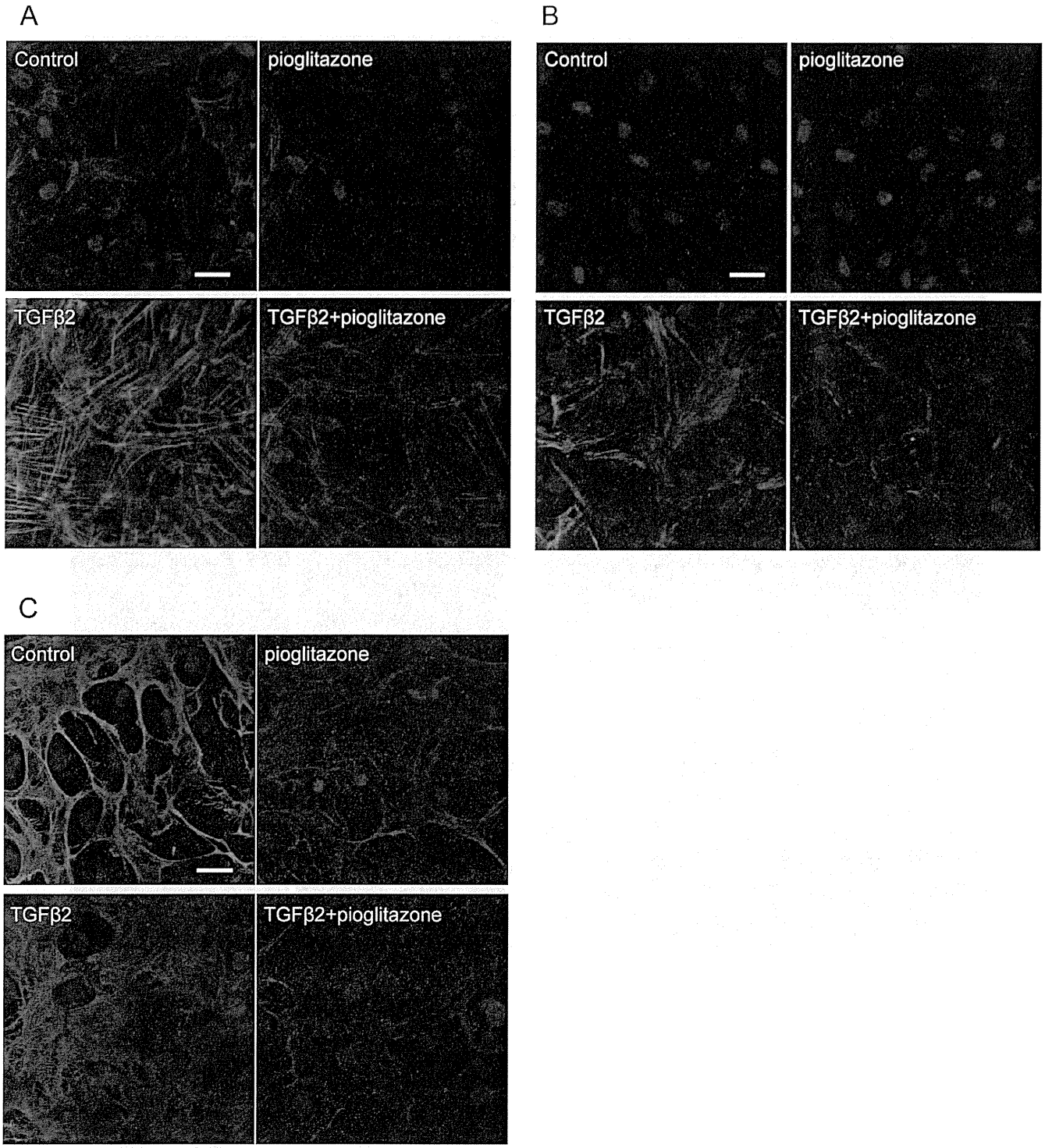


FIGURE 4. The effect of pioglitazone and TGF-β2 on the cytoskeleton of MRPECs. Images showing the immunostaining of phalloidin (**A**), αSMA (**B**), and fibronectin (**C**). *Scale bar*: 100 μm.

Next, the expression of fibrotic or EMT-related markers, such as stress fibers (Fig. 4A), α-smooth muscle actin (α-SMA, Fig. 4B), and fibronectin (Fig. 4C) was determined. The control cells demonstrated a low level of these EMT-related markers. However, the expression of these proteins was increased by exposure to TGF-β2 and that increase was reversed almost to normal control levels by the addition of PPAR-γ agonist pioglitazone.

## Effect of PPAR-γ Agonist and TGF-β2 on the Smad Pathway in MRPECs

Finally, we investigated if the Smad pathway was related to the aforementioned findings. The expression of phospho-Smad2 and phospho-Smad3 proteins was detected only faintly in the control cells (Figs. 5A, 5B); however, phosphorylation of

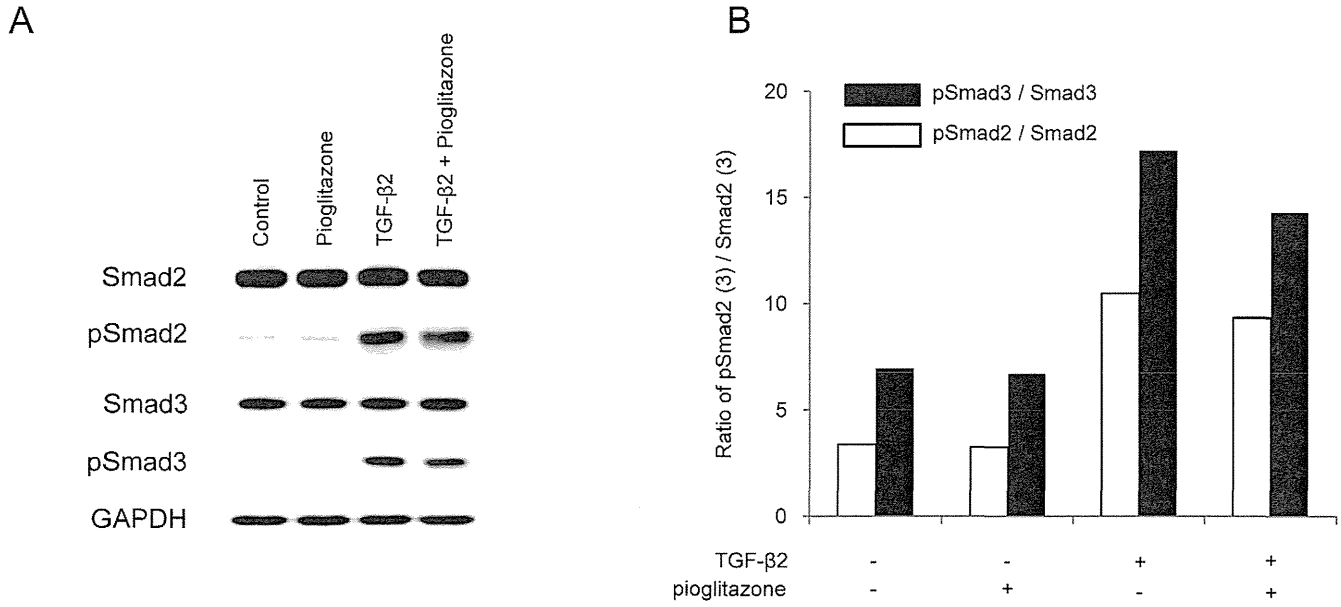


FIGURE 5. (A) The expressions of Smad2, phospho-Smad2 (pSmad2), Smad3, and pSmad3 after exposure to TGF-β2 and/or pioglitazone for 10 minutes. (B) The representative result is shown. Protein accumulation was assessed by densitometry ($n = 3$).

Smad2 and Smad3 was increased greatly in response to TGF-β2 stimulation (Figs. 5A, 5B). The PPAR-γ agonist tended to inhibit the phosphorylation of Smad2 and Smad3, yet at a low level (Fig. 5B).

## DISCUSSION

Intraocular fibrosis within a proliferative membrane is a clinically recognized underlying pathologic feature in PVR and PDR that leads to functional impairment of the retina. The proliferative membrane reportedly contains RPECs, hyalocytes, glial cells, and macrophage-derived cells,[30] and RPECs are known to have a key role in developing pathology. Numerous studies have reported the fibrotic- or EMT-like change by use of the ARPE-19 cell line, a human RPE cell line. Nonetheless, the established cell lines may have an intrinsic weakness, such as obtaining an abnormal chromosome along with passages. Thus, test results obtained through the use of these cells might not precisely mimic those of human primary cells. This concern led us to establish primate primary RPECs, similar to human primary RPECs.

TGF-β2[31] and vitreous specimens obtained from PVR or PDR[32] have been used to induce fibrotic change in ARPR-19 cells. The increased concentration of TGF-β2 in intraocular proliferative diseases is well known,[23] thus prompting us to investigate TGF-β2 as an inducer of fibrotic phase transition in our primate primary RPEC model. Fibrotic change of the primary MRPECs was observed as the accumulation of actin filaments in the cytoplasm. Overexpression of αSMA and fibronectin was detected, suggesting that TGF-β2 induces EMT-like phenotypic changes in the primary MRPECs similar to that in the human RPE cell line. These ECM proteins, major components of the proliferative membrane, are the typical pathologic features evident in intraocular proliferative diseases. Furthermore, expression of functional proteins, such as ZO-1, $Na^+/K^+$-ATPase, N-cadherin, and RPE65, was diminished at the cell surface in response to TGF-β2 stimulation. These findings suggested that we successfully made an in vitro model of an intraocular proliferative disease using primary MRPECs, and that RPECs lost the characteristic epithelial phenotypes and assumed EMT-like phenotypic changes by TGF-β2.

We further investigated the preventive effect of pioglitazone on the fibrotic- or EMT-like change induced by TGF-β2. A recent study showed that troglitazone, one of the PPAR-γ agonists, can prevent TGF-β2-induced EMT-like changes in the human RPE cell line.[33] Our results with pioglitazone, another PPAR-γ agonist, are consistent with the observation obtained from the human RPE cell line treated with troglitazone. The inhibitory effect of pioglitazone on EMT reportedly also has been observed in corneal keratocytes,[34] kidney cells,[14] and lung cells.[16] Importantly, our findings demonstrated the preventive effect of the PPAR-γ agonist pioglitazone on EMT by use of primary MRPECs. In this investigation, it is not uncovered if the effects of pioglitazone on the TGF-β2-induced EMT in cells are attributable to the PPAR-γ receptor-involved mechanism. Some of the glitazone members exhibit anti-TGF-β effects through non-PPAR-γ signaling. Thus, it is necessary to test whether or not the action reported here is via PPAR-γ. We currently are planning a future study to elucidate the molecular mechanism of the pioglitazone-mediated anti-EMT phenomenon in RPE cells, for example by using a dominant negative PPAR-γ system. The aim of our present study was to clarify the effect of PPAR-γ on the cynomolgus monkey primary RPE cells, instead of the long-term maintained cell lines. For the PPAR-γ overexpression system, it usually is necessary to use stable cell lines to investigate the intracellular events.

EMT can be induced or regulated by various growth and differentiation factors, including TGF-β, fibroblast growth factor, hepatic growth factor, and Wnt and Notch proteins.[35] Intracellular signaling molecules, such as p38 MAP kinase,[36] Notch,[37] Wnt,[38] NF-κB,[39] and phosphatidylinositol-3-OH kinase,[40] also reportedly are involved in the TGF-β signaling pathway. In the Smad pathway, after TGF-β binds to the receptor, the complex of phosphorylated Smad2/3 and Smad4 is translocated into the cell nucleus following gene overexpression in genes, such as *COL1A1*.[41] Of interest, our findings demonstrated that pioglitazone hampers phosphorylation of Smad2/3 activated by TGF-β2 in primate primary RPECs, yet at a low level. However, the precise mechanism by which pioglitazone induces the suppression of EMT in primate primary RPECs has yet to be elucidated.

The findings of our present study demonstrated that pioglitazone, a drug now being used for the treatment of diabetes mellitus, may hold the potential of being a clinically applicable pharmaceutic agent for the prevention or inhibition of intraocular proliferative diseases in the early stage of the pathology or if applied following surgery for retinal detachment. Further investigation using PVR, PDR, and AMD in vivo models is crucial to elucidate the pathology of these diseases and to discover clinically applicable therapeutic interventions for these diseases. Such future investigations hopefully will lead to the development of new drugs, such as pioglitazone.

## Acknowledgments

Yuji Sakamoto provided the monkey eyeball used in this study and John Bush reviewed the manuscript.

## References

1. Fong DS, Aiello L, Gardner TW, et al. Diabetic retinopathy. *Diabetes Care*. 2003;26(suppl 1):S99–S102.
2. Pastor JC, de la Rua ER, Martin F. Proliferative vitreoretinopathy: risk factors and pathobiology. *Prog Retin Eye Res*. 2002; 21:127–144.
3. Richter-Mueksch S, Stur M, Stifter E, Radner W. Differences in reading performance of patients with drusen maculopathy and subretinal fibrosis after CNV. *Graefes Arch Clin Exp Ophthalmol*. 2006;244:154–162.
4. Unver YB, Yavuz GA, Bekiroglu N, Presti P, Li W, Sinclair SH. Relationships between clinical measures of visual function and anatomic changes associated with bevacizumab treatment for choroidal neovascularization in age-related macular degeneration. *Eye (Lond)*. 2009;23:453–460.
5. Antonetti DA, Klein R, Gardner TW. Diabetic retinopathy. *N Engl J Med*. 2012;366:1227–1239.
6. Pastor JC. Proliferative vitreoretinopathy: an overview. *Surv Ophthalmol*. 1998;43:3–18.
7. Iwano M, Plieth D, Danoff TM, Xue C, Okada H, Neilson EG. Evidence that fibroblasts derive from epithelium during tissue fibrosis. *J Clin Invest*. 2002;110:341–350.
8. Schnaper HW, Hayashida T, Hubchak SC, Poncelet AC. TGF-beta signal transduction and mesangial cell fibrogenesis. *Am J Physiol Renal Physiol*. 2003;284:F243–F252.
9. Willis BC, Borok Z. TGF-beta-induced EMT: mechanisms and implications for fibrotic lung disease. *Am J Physiol Lung Cell Mol Physiol*. 2007;293:L525–L534.
10. Gressner AM, Weiskirchen R, Breitkopf K, Dooley S. Roles of TGF-beta in hepatic fibrosis. *Front Biosci*. 2002;7:d793–d807.
11. Piek E, Moustakas A, Kurisaki A, Heldin CH, ten Dijke P. TGF-(beta) type I receptor/ALK-5 and Smad proteins mediate epithelial to mesenchymal transdifferentiation in NMuMG breast epithelial cells. *J Cell Sci*. 1999;112(Pt 24):4557–4568.
12. Valcourt U, Kowanetz M, Niimi H, Heldin CH, Moustakas A. TGF-beta and the Smad signaling pathway support transcriptomic reprogramming during epithelial-mesenchymal cell transition. *Mol Biol Cell*. 2005;16:1987–2002.
13. Kawai T, Masaki T, Doi S, et al. PPAR-gamma agonist attenuates renal interstitial fibrosis and inflammation through reduction of TGF-beta. *Lab Invest*. 2009;89:47–58.
14. Higashi K, Oda T, Kushiyama T, et al. Additive antifibrotic effects of pioglitazone and candesartan on experimental renal fibrosis in mice. *Nephrology (Carlton)*. 2010;15:327–335.
15. Galli A, Crabb DW, Ceni E, et al. Antidiabetic thiazolidinediones inhibit collagen synthesis and hepatic stellate cell activation in vivo and in vitro. *Gastroenterology*. 2002;122: 1924–1940.
16. Aoki Y, Maeno T, Aoyagi K, et al. Pioglitazone, a peroxisome proliferator-activated receptor gamma ligand, suppresses bleomycin-induced acute lung injury and fibrosis. *Respiration*. 2009;77:311–319.
17. Wu M, Melichian DS, Chang E, Warner-Blankenship M, Ghosh AK, Varga J. Rosiglitazone abrogates bleomycin-induced scleroderma and blocks profibrotic responses through peroxisome proliferator-activated receptor-gamma. *Am J Pathol*. 2009;174:519–533.
18. Shiomi T, Tsutsui H, Hayashidani S, et al. Pioglitazone, a peroxisome proliferator-activated receptor-gamma agonist, attenuates left ventricular remodeling and failure after experimental myocardial infarction. *Circulation*. 2002;106: 3126–3132.
19. Chen S, Jim B, Ziyadeh FN. Diabetic nephropathy and transforming growth factor-beta: transforming our view of glomerulosclerosis and fibrosis build-up. *Semin Nephrol*. 2003;23:532–543.
20. Hills CE, Squires PE. TGF-beta1-induced epithelial-to-mesenchymal transition and therapeutic intervention in diabetic nephropathy. *Am J Nephrol*. 2010;31:68–74.
21. Hill C, Flyvbjerg A, Gronbaek H, et al. The renal expression of transforming growth factor-beta isoforms and their receptors in acute and chronic experimental diabetes in rats. *Endocrinology*. 2000;141:1196–1208.
22. Cheng J, Grande JP. Transforming growth factor-beta signal transduction and progressive renal disease. *Exp Biol Med (Maywood)*. 2002;227:943–956.
23. Connor TB Jr, Roberts AB, Sporn MB, et al. Correlation of fibrosis and transforming growth factor-beta type 2 levels in the eye. *J Clin Invest*. 1989;83:1661–1666.
24. Hirase K, Ikeda T, Sotozono C, Nishida K, Sawa H, Kinoshita S. Transforming growth factor beta2 in the vitreous in proliferative diabetic retinopathy. *Arch Ophthalmol*. 1998;116:738–741.
25. Bochaton-Piallat ML, Kapetanios AD, Donati G, Redard M, Gabbiani G, Pournaras CJ. TGF-beta1, TGF-beta receptor II and ED-A fibronectin expression in myofibroblast of vitreoretinopathy. *Invest Ophthalmol Vis Sci*. 2000;41:2336–2342.
26. Dunn KC, Aotaki-Keen AE, Putkey FR, Hjelmeland LM. ARPE-19, a human retinal pigment epithelial cell line with differentiated properties. *Exp Eye Res*. 1996;62:155–169.
27. Kimoto K, Nakatsuka K, Matsuo N, Yoshioka H. p38 MAPK mediates the expression of type I collagen induced by TGF-beta 2 in human retinal pigment epithelial cells ARPE-19. *Invest Ophthalmol Vis Sci*. 2004;45:2431–2437.
28. Maminishkis A, Chen S, Jalickee S, et al. Confluent monolayers of cultured human fetal retinal pigment epithelium exhibit morphology and physiology of native tissue. *Invest Ophthalmol Vis Sci*. 2006;47:3612–3624.
29. Parapuram SK, Chang B, Li L, et al. Differential effects of TGFbeta and vitreous on the transformation of retinal pigment epithelial cells. *Invest Ophthalmol Vis Sci*. 2009;50:5965–5974.
30. Oberstein SY, Byun J, Herrera D, Chapin EA, Fisher SK, Lewis GP. Cell proliferation in human epiretinal membranes: characterization of cell types and correlation with disease condition and duration. *Mol Vis*. 2011;17:1794–1805.
31. Saika S, Yamanaka O, Ikeda K, et al. Inhibition of p38MAP kinase suppresses fibrotic reaction of retinal pigment epithelial cells. *Lab Invest*. 2005;85:838–850.
32. Casaroli-Marano RP, Pagan R, Vilaro S. Epithelial-mesenchymal transition in proliferative vitreoretinopathy: intermediate filament protein expression in retinal pigment epithelial cells. *Invest Ophthalmol Vis Sci*. 1999;40:2062–2072.
33. Cheng HC, Ho TC, Chen SL, Lai HY, Hong KF, Tsao YP. Troglitazone suppresses transforming growth factor beta-

mediated fibrogenesis in retinal pigment epithelial cells. *Mol Vis*. 2008;14:95–104.

34. Pan H, Chen J, Xu J, Chen M, Ma R. Antifibrotic effect by activation of peroxisome proliferator-activated receptor-gamma in corneal fibroblasts. *Mol Vis*. 2009;15:2279–2286.
35. Moustakas A, Heldin CH. Signaling networks guiding epithelial-mesenchymal transitions during embryogenesis and cancer progression. *Cancer Sci*. 2007;98:1512–1520.
36. Zavadil J, Bottinger EP. TGF-beta and epithelial-to-mesenchymal transitions. *Oncogene*. 2005;24:5764–5774.
37. Zavadil J, Cermak L, Soto-Nieves N, Bottinger EP. Integration of TGF-beta/Smad and Jagged1/Notch signalling in epithelial-to-mesenchymal transition. *EMBO J*. 2004;23:1155–1165.
38. Masszi A, Fan L, Rosivall L, et al. Integrity of cell-cell contacts is a critical regulator of TGF-beta 1-induced epithelial-to-myofibroblast transition: role for beta-catenin. *Am J Pathol*. 2004; 165:1955–1967.
39. Huber MA, Azoitei N, Baumann B, et al. NF-kappaB is essential for epithelial-mesenchymal transition and metastasis in a model of breast cancer progression. *J Clin Invest*. 2004;114: 569–581.
40. Bakin AV, Tomlinson AK, Bhowmick NA, Moses HL, Arteaga CL. Phosphatidylinositol 3-kinase function is required for transforming growth factor beta-mediated epithelial to mesenchymal transition and cell migration. *J Biol Chem*. 2000; 275:36803–36810.
41. Burch ML, Zheng W, Little PJ. Smad linker region phosphorylation in the regulation of extracellular matrix synthesis. *Cell Mol Life Sci*. 2011;68:97–107.

PLOS | ONE

# HLA-A*0206 with TLR3 Polymorphisms Exerts More than Additive Effects in Stevens-Johnson Syndrome with Severe Ocular Surface Complications

**Mayumi Ueta[1,2]*, Katsushi Tokunaga[3], Chie Sotozono[1], Hiromi Sawai[3], Gen Tamiya[4], Tsutomu Inatomi[1], Shigeru Kinoshita[1]**

**1** Department of Ophthalmology, Kyoto Prefectural University of Medicine, Kyoto, Japan, **2** Research Center for Inflammation and Regenerative Medicine, Faculty of Life and Medical Sciences, Doshisha University, Kyoto, Japan, **3** Department of Human Genetics, Graduate School of Medicine, University of Tokyo, Tokyo, Japan, **4** Advanced Molecular Epidemiology Research Institute, Faculty of Medcine, Yamagata University, Yamagata, Japan

## Abstract

***Background:*** Stevens-Johnson syndrome (SJS) is an acute inflammatory vesiculobullous reaction of the skin and mucosa, often including the ocular surface, and toxic epidermal necrolysis (TEN) occurs with its progression. Although SJS/TEN is thought to be initiated by certain types of medication coupled with possible infection. In the present study we examined the multiplicative interaction(s) between HLA-A*0206 and 7 Toll-like receptor 3 (TLR3) Single-nucleotide polymorphisms (SNPs) in patients with SJS/TEN.

***Principal Findings:*** We analyzed the genotypes for HLA-A and 7 TLR3 SNPs in 110 Japanese SJS/TEN patients with severe ocular complications and 206 healthy volunteers to examine the interactions between the two loci. We found that HLA-A*0206 exhibited a high odds ratio for SJS/TEN (carrier frequency: OR = 5.1; gene frequency: OR = 4.0) and that there was a strong association with TLR3 rs.5743312T/T SNP (OR = 7.4), TLR3 rs.3775296T/T SNP (OR = 5.8), TLR3 rs.6822014G/G SNP (OR = 4.8), TLR3 rs.3775290A/A SNP (OR = 2.9), TLR3 rs.7668666A/A SNP (OR = 2.7), TLR3 rs.4861699G/G SNP (OR = 2.3), and TLR3 rs.11732384G/G SNP (OR = 1.9). There was strong linkage disequilibrium (LD) between rs.3775296 and rs.5743312 and between rs.7668666 and rs.3775290. The results of interaction analysis showed that the pair, HLA-A*0206 and TLR3 SNP rs3775296T/T, which exhibited strong LD with TLR3 rs.5743312, exerted more than additive effects (OR = 47.7). The other pairs, HLA-A*0206 and TLR3 rs.3775290A/A SNP (OR = 11.4) which was in strong LD with TLR3 rs7668666A/A SNP, and TLR3 rs4861699G/G SNP (OR = 7.6) revealed additive effects. Moreover, the combination HLA-A*0206 and TLR3 rs3775296T/T was stronger than the TLR3 rs6822014G/G and TLR3 rs3775290A/A pair, which reflected the interactions within the TLR3 gene alone.

***Significance:*** By interaction analysis, HLA-A*0206 and TLR3 SNP rs3775296T/T, which were in strong LD with TLR3 SNP rs5743312T/T, manifested more than additive effects that were stronger than the interactions within the TLR3 gene alone. Therefore, multiplicative interactions of HLA-A and TLR3 gene might be required for the onset of SJS/TEN with ocular complications.

**Citation:** Ueta M, Tokunaga K, Sotozono C, Sawai H, Tamiya G, et al. (2012) HLA-A*0206 with TLR3 Polymorphisms Exerts More than Additive Effects in Stevens-Johnson Syndrome with Severe Ocular Surface Complications. PLoS ONE 7(8): e43650. doi:10.1371/journal.pone.0043650

**Editor:** Yoshihiko Hoshino, National Institute of Infectious Diseases, Japan

**Received** April 2, 2012; **Accepted** July 24, 2012; **Published** August 17, 2012



**Funding:** This work was supported in part by grants-in-aid for scientific research from the Japanese Ministry of Health, Labour and Welfare, the Japanese Ministry of Education, Culture, Sports, Science and Technology, a research grant from the Kyoto Foundation for the Promotion of Medical Science, and the Intramural Research Fund of Kyoto Prefectural University of Medicine. The funders had no role in study design, data collection and analysis, decision to publish, or preparation of the manuscript.

**Competing Interests:** The authors have declared that no competing interests exist.

* E-mail: mueta@koto.kpu-m.ac.jp

## Introduction

Stevens-Johnson syndrome (SJS) is an acute inflammatory vesiculobullous reaction of the skin and mucous membranes. It was first described in 1922 by Stevens and Johnson, [1] both pediatricians, who encountered 2 boys aged 8 and 7 who manifested an extraordinary, generalized skin eruption, persistent fever, inflamed buccal mucosa, and severe purulent conjunctivitis resulting in marked visual disturbance. Subsequently, other pediatricians reported that SJS was associated with infectious agents such as *Mycoplasma pneumoniae*, [2] and a viral etiology involving herpes simplex virus, Epstein-Barr virus, cytomegalovirus, and varicella zoster virus [3]. On the other hand, dermatologists claimed that more than 100 different drugs were implicated in eliciting SJS and its severe form, toxic epidermal necrolysis (TEN) [4,5]. The annual incidence of SJS and TEN has been estimated to be 0.4–1 and 1–6 cases per million persons, respectively; [6,7] the reported mortality rate is 3% and 27%, respectively [8]. Although rare, these reactions have high morbidity and mortality rates, and often result in severe and definitive sequelae such as vision loss. SJS/TEN is one of the most devastating ocular surface diseases leading to corneal damage and

loss of vision. The reported incidence of ocular complications in SJS/TEN is 50–68% [7,8].

In the acute stage, patients manifest vesiculobullous lesions of the skin and mucosa, especially that of the eyes and mouth, and severe conjunctivitis. The loss of finger nails in the acute or subacute stage due to paronychia was observed, has been observed in almost all SJS/TEN patients with severe ocular surface complications [9,10,11,12].

In the chronic stage, despite healing of the skin lesions, ocular surface complications such as conjunctival invasion into the cornea [10,11,12,13,14,15,16,17,18]. It is also reported that lid margin keratinization and tarsal scarring, together with lipid tear deficiency, contributes to corneal complications because of blink-related microtrauma [19].

Elsewhere we reported that the frequency of carriers of the HLA-A*0206 antigen is significantly higher among Japanese patients with severe ocular surface complications than in other populations [18,20]. Our single nucleotide polymorphism (SNP) association analysis of candidate genes documented the associated polymorphisms of several immune-related genes including *TLR3*, [12,17] *IL4R*, [14,16] *IL13*, [16] and *FasL* [15]in Japanese SJS/TEN patients with severe ocular surface complications. To elucidate the detailed pathophysiology of SJS/TEN we performed a genome-wide association study of SJS/TEN patients and found associations between 6 SNPs in the prostaglandin E receptor 3 (EP3) gene (*PTGER3*) and SJS/TEN accompanied by severe ocular surface complications [11]. Moreover, gene-gene interaction analysis in SJS/TEN patients with severe ocular surface complications revealed that the interaction between *TLR3* and *PTGER3* exerted SJS/TEN susceptibility effects, and there was a functional interaction between TLR3 and EP3 in a murine experimental allergic conjunctivitis model. [12].

In the present study we examined the multiplicative interaction(s) between HLA-A*0206 and 7 TLR3 SNPs (rs3775296 (uSNP), rs5743312 (iSNP), rs6822014 (gSNP), rs3775290 (sSNP), rs7668666 (iSNP), rs11732384 (iSNP), and rs4861699 (gSNP)) associated with the SJS/TEN patients [12,17] as the onset of SJS/TEN was associated not only with the administration of drugs but also with putative viral syndromes [10,11,12,17]. HLA-A is a component of HLA class I, which resides on the surface of all nucleated cells and alerts the immune system that the cell may be infected by a virus, thereby targeting the cell for destruction. TLR3 recognises viral double-stranded RNA [21].

## Results

We analyzed the genotypes for HLA-A and 7 TLR3 SNPs in 110 Japanese SJS/TEN patients with severe ocular complications and 206 healthy volunteers to examine the interactions between the two loci.

We found that HLA-A*0206 exhibited a high odds ratio for SJS/TEN (carrier frequency: $p = 6.9\times10^{-10}$, OR = 5.1; gene frequency: $p = 2.5\times10^{-9}$, OR = 4.0) (Table 1).

We also found that there was a strong association with TLR3 rs.5743312T/T SNP (T/T vs T/C+C/C: $p = 2.5\times10^{-6}$, OR = 7.4), TLR3 rs.3775296T/T SNP (T/T vs T/G+G/G: $p = 8.2\times10^{-6}$, OR = 5.8), TLR3 rs.6822014G/G SNP (G/G vs G/A+A/A: $p = 1.2\times10^{-4}$, OR = 4.8), TLR3 rs.3775290A/A SNP (A/A vs A/G+G/G: $p = 7.1\times10^{-4}$, OR = 2.9), TLR3 rs.7668666A/A SNP (A/A vs A/G+G/G: $p = 1.2\times10^{-3}$, OR = 2.7), TLR3 rs.4861699G/G SNP (G/G vs G/A+A/A:

**Table 1.** Association between HLA-A*0206 and SJS/TEN with ocular complications.

| HLA-A | Carrier frequency | | | | Gene frequency | | | |
|---|---|---|---|---|---|---|---|---|
| | SJS (n = 110) | Normal (n = 206) | p-value ($\chi^2$) | Odds Ratio | SJS (n = 220) | Normal (n = 412) | p-value ($\chi^2$) | Odds Ratio |
| *0206 | 46.4% (51/110) | 14.6% (30/206) | $6.9\times10^{-10}$ | 5.07 | 24.1% (53/220) | 7.3% (30/412) | $2.5\times10^{-9}$ | 4.04 |
| *0101 | 0% (0/110) | 1.4% (3/206) | 0.2 | – | 0% (0/220) | 0.7% (3/412) | 0.2 | – |
| *0201 | 26.4% (29/110) | 21.4% (44/206) | 0.3 | – | 14.5% (32/220) | 11.4% (47/412) | 0.3 | – |
| *0207 | 9.1% (10/110) | 7.8% (16/206) | 0.7 | – | 4.5% (10/220) | 3.9% (16/412) | 0.7 | – |
| *0210 | 0% (0/110) | 1.0% (2/206) | 0.3 | – | 0% (0/220) | 0.5% (2/412) | 0.3 | – |
| *0301 | 2.7% (3/110) | 1.4% (3/206) | 0.4 | – | 1.4% (3/220) | 0.7% (3/412) | 0.4 | – |
| *0302 | 0% (0/110) | 0.5% (1/206) | 0.5 | – | 0% (0/220) | 0.2% (1/412) | 0.5 | – |
| *1101 | 7.3% (8/110) | 18.4% (38/206) | $7.3\times10^{-3}$ | 0.35 | 3.6% (8/220) | 9.2% (38/412) | $1.0\times10^{-2}$ | 0.37 |
| *1102 | 0% (0/110) | 0.5% (1/206) | 0.5 | – | 0% (0/220) | 0.2% (1/412) | 0.5 | – |
| *2402 | 45.5% (50/110) | 60.7% (125/206) | $9.5\times10^{-3}$ | 0.54 | 25.0% (55/220) | 36.7% (151/412) | $2.9\times10^{-3}$ | 0.58 |
| *2420 | 0% (0/110) | 0.5% (1/206) | 0.5 | – | 0% (0/220) | 0.2% (1/412) | 0.5 | – |
| *2601 | 9.1% (10/110) | 12.6% (26/206) | 0.3 | – | 4.5% (10/220) | 6.6% (27/412) | 0.3 | – |
| *2602 | 5.5% (6/110) | 2.9% (6/206) | 0.3 | – | 2.7% (6/220) | 1.7% (7/412) | 0.4 | – |
| *2603 | 1.8% (2/110) | 7.8% (16/206) | $3.0\times10^{-2}$ | 0.2 | 0.9% (2/220) | 3.9% (16/412) | $3.2\times10^{-2}$ | 0.2 |
| *2605 | 0% (0/110) | 0.5% (1/206) | 0.5 | – | 0% (0/220) | 0.2% (1/412) | 0.5 | – |
| *2901 | 0% (0/110) | 1.9% (4/206) | 0.1 | – | 0% (0/220) | 1.0% (4/412) | 0.1 | – |
| *3001 | 0.9% (1/110) | 0% (0/206) | 0.2 | – | 0.5% (1/220) | 0% (0/412) | 0.2 | – |
| *3101 | 13.6% (15/110) | 16.5% (34/206) | 0.5 | – | 6.8% (15/220) | 8.3% (34/412) | 0.5 | – |
| *3201 | 0% (0/110) | 0.5% (1/206) | 0.5 | – | 0% (0/220) | 0.2% (1/412) | 0.5 | – |
| *3303 | 22.7% (25/110) | 14.1% (29/206) | 0.05 | – | 11.4% (25/220) | 7.0% (29/412) | 0.06 | – |

doi:10.1371/journal.pone.0043650.t001

**Table 2.** Association between TLR3 SNPs and SJS/TEN with ocular complications.

| rs number of SNP | Genotypes | | Case (N = 110) | Control (N = 206) | Allele 1 vs. Allele 2 | Genotype 11 vs. 12+22 | Genotype 11+12 vs. 22 |
|---|---|---|---|---|---|---|---|
| | | | | | P-value[a] | P-value[a] | P-value[a] |
| | | | | | OR[b] | OR[b] | OR[b] |
| | | | | | (95%CI[c]) | (95%CI[c]) | (95%CI[c]) |
| rs4861699 | 11 | G/G | 65/110 (59.1%) | 79/206 (38.3%) | 0.0016 | $4.2\times10^{-4}$ | 0.28 |
| | 12 | G/A | 36/110 (32.7%) | 102/206 (49.5%) | 1.80 | 2.32 | 1.55 |
| | 22 | A/A | 9/110 (8.2%) | 25/206 (12.1%) | (1.25–2.59) | (1.45–3.72) | (0.70–3.45) |
| rs6822014 | 11 | A/A | 55/110 (50.0%) | 127/206 (61.7%) | $8.9\times10^{-4}$ | 0.046 | $1.2\times10^{-4}$ |
| | 12 | A/G | 37/110 (33.6%) | 71/206 (34.5%) | 0.54 | 0.62 | 0.21 |
| | 22 | G/G | 18/110 (16.4%) | 8/206 (3.9%) | (0.37–0.78) | (0.39–0.99) | (0.09–0.49) |
| rs11732384 | 11 | G/G | 72/110 (65.5%) | 103/206 (50.0%) | 0.029 | 0.0085 | 0.88 |
| | 12 | G/A | 31/110 (28.2%) | 89/206 (43.2%) | 1.54 | 1.89 | 1.07 |
| | 22 | A/A | 7/110 (6.4%) | 14/206 (6.8%) | (1.04–2.28) | (1.17–3.06) | (0.42–2.74) |
| rs3775296 | 11 | G/G | 49/110 (44.5%) | 109/206 (52.9%) | 0.0020 | 0.16 | $8.2\times10^{-6}$ |
| | 12 | G/T | 40/110 (36.4%) | 89/206 (43.2%) | 0.58 | 0.71 | 0.17 |
| | 22 | T/T | 21/110 (19.1%) | 8/206 (3.9%) | (0.40–0.82) | (0.45–1.14) | (0.07–0.40) |
| rs5743312 | 11 | C/C | 52/110 (47.3%) | 115/206 (55.8%) | 0.0014 | 0.15 | $2.5\times10^{-6}$ |
| | 12 | C/T | 38/110 (34.5%) | 85/206 (41.3%) | 0.56 | 0.71 | 0.14 |
| | 22 | T/T | 20/110 (18.2%) | 6/206 (2.9%) | (0.39–0.80) | (0.45–1.13) | (0.05–0.35) |
| rs7668666 | 11 | C/C | 36/110 (32.7%) | 83/206 (40.3%) | 0.0085 | 0.19 | 0.0012 |
| | 12 | C/A | 47/110 (42.7%) | 101/206 (49.0%) | 0.64 | 0.72 | 0.37 |
| | 22 | A/A | 27/110 (24.5%) | 22/206 (10.7%) | (0.46–0.89) | (0.44–1.17) | (0.20–0.68) |
| rs3775290 | 11 | G/G | 38/110 (34.5%) | 82/206 (39.8%) | 0.016 | 0.36 | $7.1\times10^{-4}$ |
| | 12 | G/A | 45/110 (40.9%) | 103/206 (50.0%) | 0.66 | 0.80 | 0.35 |
| | 22 | A/A | 27/110 (24.5%) | 21/206 (10.2%) | (0.48–0.93) | (0.50–1.29) | (0.18–0.65) |

[a]*P*-value for allele or genotype frequency comparisons between cases and controls using the chi-square test.
[b]OR, odds ratio.
[c]CI, confidence interval.
doi:10.1371/journal.pone.0043650.t002

$p = 4.2\times10^{-4}$, OR = 2.3), and TLR3 rs.11732384G/G SNP (G/G vs G/A+A/A: $p = 8.5\times10^{-3}$, OR = 1.9) (Table 2). All SNPs were in Hardy-Weinberg equilibrium ($p>0.01$) in the samples from patients and the controls. Based on the squared correlation coefficient $r^2$, we investigated the linkage disequilibrium (LD) among the *TLR3* SNPs. We found strong LD between rs.3775296 and rs.5743312 (D' = 1, $r^2 = 0.911$), and between rs.7668666 and rs.3775290 (D' = 0.973, $r^2 = 0.934$) (Fig. 1).

Results of interaction analysis showed that the pair, HLA-A*0206 and TLR3 SNP rs3775296T/T, which exhibited strong LD with TLR3 rs.5743312, exerted more than additive effects. We found that while 11 of the 110 patients (10%) manifested both HLA-A*0206 and TLR3 rs3775296T/T SNP, none of the 206 controls did ($p = 6.5\times10^{-6}$, OR = 47.7, Woolf's correction). The other pairs, HLA-A*0206 and TLR3 rs.3775290A/A SNP, which was in strong LD with TLR3 rs.7668666, or TLR3 rs4861699G/G SNP revealed additive effects: 16 of the 110 patients (14.5%) but only 3 of the 206 controls (1.5%) had both HLA-A*0206 and TLR3 rs.3775290A/A SNP ($p = 7.4\times10^{-6}$, OR = 11.4). In addition, 33 of the 110 patients (30%), compared to 11 of the 206 controls (5.3%), had both HLA-A*0206 and TLR3 rs.4861699G/G SNP ($p = 1.6\times10^{-9}$, OR = 7.6) (Table 3).

Moreover, to examine the interactions within the TLR3 gene alone we analyzed interactions between 2 each of 5 TLR3 SNPs (rs3775296, rs6822014, rs3775290, rs11732384, rs4861699). Combinations of high risk genotypes, on which the observed numbers in cases were greater than of the controls and greater than five, were analyzed. One of the 9 combinations, TLR3 rs6822014G/G and TLR3 rs3775290A/A, exerted more than additive effects (OR 16.1, $p = 2.0\times10^{-6}$) (Table 4). However, the combination HLA-A*0206 and TLR3 rs3775296T/T produced a stronger additive effect than it. In addition, we performed haplotype association analysis with the 7 TLR3 SNPs (rs4861699, rs6822014, rs11732384, rs3775296, rs5743312, rs7668666, rs3775290) and the 5 TLR3 SNPs (rs4861699, rs6822014, rs11732384, rs3775296, rs3775290), and found that no haplotype showed strong association ($p<0.001$) (Table S1). Thus, the haplotype associations appear to contribute little to the observed interactions.

## Discussion

To our knowledge, ours is the first report documenting the additive effects of HLA-A*0206 and TLR3 polymorphisms. Our interaction analysis showed that the pair HLA-A*0206 and TLR3 SNP rs3775296T/T, which was in strong LD with TLR3 rs.5743312, exerted more than additive effects, and that other pairs, HLA-A*0206 and TLR3 rs.3775290A/A SNP in strong LD